ISSN 0869-5938, Stratigraphy and Geological Correlation, 2023, Vol. 31, No. 3, pp. 109–134. © Pleiades Publishing, Ltd., 2023.
Russian Text © The Author(s), 2023, published in Stratigrafiya, Geologicheskaya Korrelyatsiya, 2023, Vol. 31, No. 3, pp. 3–31.

Dedicated to memory of S.D. Chervyakovskiy

Vodorazdelny Granitic Pluton, Subpolar Urals, and Problems of Correlation of Pre-Ordovician Granitoids and Volcanic Rocks of the Northern Part of the Lyapin Anticlinorium

G. Yu. Shardakova[a], *, E. N. Volchek[a], V. S. Chervyakovskiy[a], M. V. Chervyakovskaya[a], and V. V. Kholodnov[a]

[a] *Institute of Geology and Geochemistry, Ural Branch, Russian Academy of Sciences, Yekaterinburg, 620010 Russia*
**e-mail: shardakovagalina@mail.ru*

Received July 16, 2022; revised August 4, 2022; accepted October 19, 2022

Abstract—The petrochemical features of granites of the Vodorazdelny pluton (Subpolar Urals, Lyapin Anticlinorium) indicate that these suprasubduction rocks are similar to I-granites. The ratios of key elements (Rb, Ba, Th, Sr, Y, and Nb) suggest that mafic rocks of a melting slab and fluid related to their dehydration could have been involved in the generation of granites. The U–Pb age of the main population of igneous zircons of 593 ± 4 Ma corresponds to the Vendian (Ediacaran) and coincides with the age of granites of the nearby Vangyr pluton (598 ± 5 Ma), as well as the age of cores of zircons from granites of the Kozhim pluton in the north. The $\varepsilon_{Hf}(t)$ values (from –2 to 0) of igneous zircons with the age corresponding to the age of granites of the Vodorazdelny pluton indicate a heterogeneous melt source. The petrogeochemical and isotopic-geochronological parameters of granites (as well as zircons) are inconsistent with the attribution of the Vodorazdelny pluton (and analogous Vangyr and Kozhim plutons) to the Cambrian Salner–Mankhambo complex and indicate the recognition of a possible Vendian (?) complex with the age of ~598 Ma during the geological survey. The presence of Middle Riphean–Vendian–Cambrian stages of granite formation in the Lyapin Anticlinorium and related metamorphism and a complex composition of ancient metamorphic sequences in the basement of this structure are responsible for the varying isotopic parameters characterizing the heterogeneous melt source, on one hand, and a convergent series of geochemical features, on the other hand.

Keywords: Subpolar Urals, Vendian, granites, zircons, isotopy, accretion, subduction, plume

DOI: 10.1134/S0869593823030073

INTRODUCTION

The petrogeochemical features and isotopic-geochronological parameters of granitoids, which are an important constituent of the upper part of the crust, could correct the ideas on deep geodynamics of magmatic processes. The analysis of published and geological survey literature shows that there are poorly studied objects in the world, the classification of which cannot be supported by sufficient data (Soboleva, 2001; Pystin and Pystina, 2011; Puchkov, 2018; Kholodnov et al., 2022). These "white spots" are especially abundant in areas with complex structures, e.g., accretionary zones, which contain blocks of various compositions and origins. The examples of the accretionary structures include blocks which are located to the west of the Main Uralian Fault Zone, Bolshaya Zemlya (Bolshezemel'skaya) in the Subpolar Urals, and a series of the southernmost blocks (Fig. 1b). These blocks host abundant Cambrian–Paleozoic sedimentary rocks and their basement includes volcano-sedimentary and metamorphic rocks with intrusions of ultramafic rocks (rare), gabbroids, and granitoids.

The pre-Ordovician complexes, which are part of the structure of the present-day Uralian Orogen and its western frame, are termed proto- or pre-Uralides (Puchkov, 2000; Kuznetsov et al., 2007). They are exposed in the Central Uralian Uplift and form a longitudinal band no less than 2000 km long. The Lyapin Anticlinorium in the north spans the Subpolar and North Uralian segments of the Central Uralian Uplift. The anticlinorium includes the Mankhambo (south) and Kozhim (north) blocks, which are divided by large transverse faults and, according to the opinion of some researchers (Volchek, 2004; Kholodnov et al., 2022), could have evolved asynchronously. The igneous rocks of this structure are characterized in detail in numerous

Fig. 1. Position of studied objects in structures of the Urals and its frame. (a) Position of the Uralian fold belt on a map of Russia, (b) tectonic scheme of the Urals and its frame with the location of the studied objects, modified after (Puchkov, 2000; Kuznetsov et al., 2007). Fault zones: PIC, Pechora–Ilych–Chiksha Zone; MUF, Main Uralian Fault. Structures and megazones: I, East European Platform; II, III, Timan Megablock: Timan (II) and Izhem (III) zones; IV, V, Pechora Megablock: Pechora (IV) and Bolshaya Zemlya (V) zones; VI, VII, East Uralian Megazone: unspecified Tagil and Magnitogorsk zones (VI); East Uralian Uplift Zone (VII); VIII, West Siberian Platform. Blocks with ancient basement with Riphean–Vendian–Cambrian igneous rocks (from north to south): LA, Lyapin Anticlinorium; IA, Isherim Anticlinorium; KKA, Kvarkush–Kamennaya Gora (Kammenogorskii) Anticlinorium; UB, Ufalei Block; BMA, Bashkirian Meganticlinorium; UT, Uraltau Uplift Zone; LS, Lushnikovo structure. Rectangle, area of Lyapin Anticlinorium, Kozhim (north) and Mankhambo (south) blocks. (c) Geological scheme of the Lyapin Anticlinorium after (Puchkov, 2000; Kuznetsov et al., 2007; Dushin et al., 2017). (1) Mesozoic–Cenozoic complexes of the cover of the West Siberian Plate; (2) Permian–Triassic complexes of the cover of the East European Platform and Timanides; (3–8) Late Precambrian–Paleozoic complexes (pre-Uralides and Uralides) of the West Uralian Megazone: (3) Ordovician–Late Paleozoic complexes (Uralides); (4–8) Late Precambrian–Cambrian complexes (pre-Uralides): (4) volcano-sedimentary complexes (Mount Sablya Formation and its analogs); (5) metamorphosed volcano-sedimentary complexes; (6) gneiss–amphibole and gneiss–migmatite complexes; (7, 8) granitoids of I (7) and A (8) types; (9) Paleozoic volcano-sedimentary and ophiolitic complexes of the East Uralian Megazone; (10) gabbroids. Numbers in circles, granitic plutons. Kozhim Block: 1, Lemva; 2, Yarota and Bad'yus; 3, Tynagot; 4, Khatalamba–Lapchinsky; 5, Kozhim; 6, Lapchavozh; 7, Maldy; 8, Naroda; 9, Vodorazdelny; 10, Vangyr; 11, Parnuk, Mankhobeyu, Gorodkovskii; 12, Neroika–Patok; 13, Salner; 14, Nyarta; 15, Maly Patok; 16, Tynagot, Keftalyk; 17, Khartess; 18, Kulemshor, Mankhambo block; 19, Il'ya-Iz; 20, Mankhambo; 21, Sotchem'el (gabbro); 22, Torrepore-Iz; 23, Ydzhidlyaga; 24, Sys'in (not to scale). Black rectangle: position of the studied granitoids. (d) Geological map of the Vodorazdelny (I) and Vangyr (II) plutons, simplified after (Dushin et al., 2017). (1) Middle Riphean Puiva Formation: phyllitic micaceous-quartz schist with thin lenses of dolomite and quartzite; (2) Upper Riphean Khobeya Formation: quartzite, quartzitic sandstone, banded silty shale; dolomite lenses in the lower part; (3) Upper Riphean Moroya Formation: phyllitic micaceous-quartz carbonaceous schist with dolomite and marble lenses and microfossils in the lower part; (4) basaltoids of the Moroya Complex (in structure of the formation); (5) Middle Vendian–Cambrian Laptopai Formation: carbonaceous schist with interlayers of tillitic conglomerates, a horizon of olistostromes, polymictic conglomerates, and gravelites; (6) Lower Vendian Ar'yanshor Sequence: silty shale, siltstone, sandstone; variegated shale and lenses of dolomites in the upper part; (7) unspecified Lower Ordovician Obeya Formation with red quartz conglomerate, quartzitic sandstone, silty-clayey shale; (8) Quaternary sediments; (9) granite and leucogranite of the Vodorazdelny (I) and Vangyr (II) plutons; (10) faults: (a) proven; (b) inferred.

papers (Fishman and Goldin, 1963; Chervyakovskiy et al., 1992; Makhlaev, 1996; Udoratina et al., 2006, 2021; Kuznetsov et al., 2007; Pystin and Pystina, 2008; Dushin et al., 2009, 2021, 2017; Andreicheva, 2010; Soboleva, 2011, 2004). They showed the presence of A-, I-, and S-type granitoids, which locally intruded almost synchronously. The granitoids exhibit convergent features and a geodynamic regime of their intrusion within a range from 650 to 480 Ma and therefore their attribution to different complexes upon geological mapping (i.e., the correlation of granitoids of various plutons) is a matter of debate.

There are distinct models of the pre-Ordovician geodynamic evolution of the structure of the Subpolar Urals and related granitoids: riftogenic, accretionary–collision, and oceanic reviewed in details by (Kuznetsov et al., 2007; Kuznetsov, 2009; Udoratina et al., 2021). Other authors provided an original viewpoint on transform (mostly divergent) movements in the southern part of the Lyapin Anticlinorium (Mankhambo Block), which were initiated by several plume pulses, and showed a different role of oceanic and continental components in the substrate (Kholodnov et al., 2022). The Paleozoic granites of the "Uralian" evolution stage are omitted in our work; they are a subject of another study.

The object of our study includes the granites of the Vodorazdelny pluton (Kozhim Block of the Lyapin Anticlinorium) (Fig. 1), which were poorly studied and dated. A topical practical problem is the determination of their age, relations to country rocks, and attribution to other complexes upon geological mapping. The granites of the Vodorazdelny and nearby Vangyr plutons were previously included in the structure of the Paleozoic Kozhim Complex (Fishman and Goldin, 1963; Andreichev, 2010). A young age of the Vangyr granites is not supported by modern methods, and this name was deleted from geological maps (Ivanov et al., 2013a, 2013b; Dushin et al., 2017). On the basis of the U–Pb age of zircon (485 Ma, Udoratina et al., 2020), the Kozhim, Vangyr, and Vodorazdelny plutons are ascribed to the Vendian–Lower Cambrian Salner–Mankhambo (phase II) complex in the latest editions of the 1 : 200000 State Geological Map (Ivanov et al., 2013b). The data provided in our paper, however, contradict this viewpoint.

The aim of our study is the refinement of the correlation scheme and ideas on the geodynamic setting of granitic intrusion of the Lyapin Anticlinorium in the Vendian–the beginning of the Cambrian on the basis of the petrochemical data of rocks of the Vodorazdelny pluton, the peculiarities of chemical composition of their zircons, the zircon populations, their age, and the parameters of their Lu–Hf system. The results are new and original and contribute to the ideas on the classification and geodynamic setting of granitic intrusions of the Lyapin Anticlinorium of this period and can be used in geological mapping.

BRIEF GEOLOGICAL AND PETROGRAPHIC CHARACTERISTICS

The Vodorazdelny pluton is located at the interfluve of the Vangyr River and Nadezhd River (the right tributary of the Bolshoi Patok River) on the western

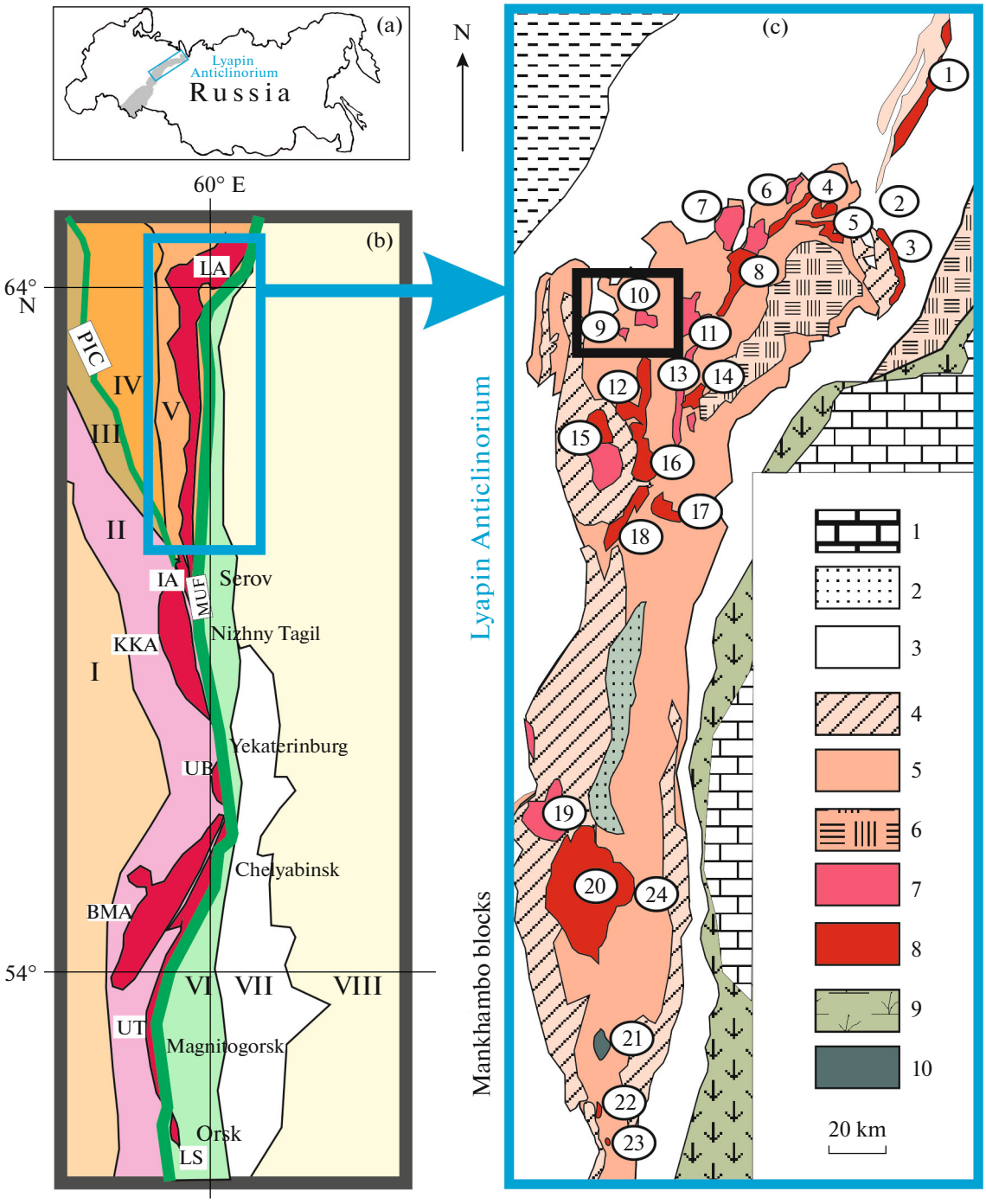

slope of the Subpolar Urals within the Kozhim Block (Figs. 1c, 1d). This pluton in plan has a pearlike morphology with a length of ~4 km and a maximum width of 2.5 km. The area of the surface outcrops is ~7 km^2. According to the estimates of Rudich (1967), the erosion level is 400–500 m. According to geophysical data, the pluton is a stock dipping to the east (60°–70°) and intruding a NE wing of the Bezymyannaya Syncline. The Vangyr pluton described in detail by Kuznetsov and Udoratina (2007) is located 2 km to the northeast of the Vodorazdelny pluton (Fig. 2), but these authors did not discuss their relations.

The Vodorazdelny pluton has a concentric-zonal structure: the quartz porphyries are replaced by porphyry granites and further by small-, medium- and coarse-grained poprhyritic granites from the periphery to the center. The rocks of this pluton in the west are surrounded by rocks of the Khobeiz (Upper Riphean) and Tel'pos (Lower Ordovician) formations (old unpublished materials) or rocks of the Khobeyu,

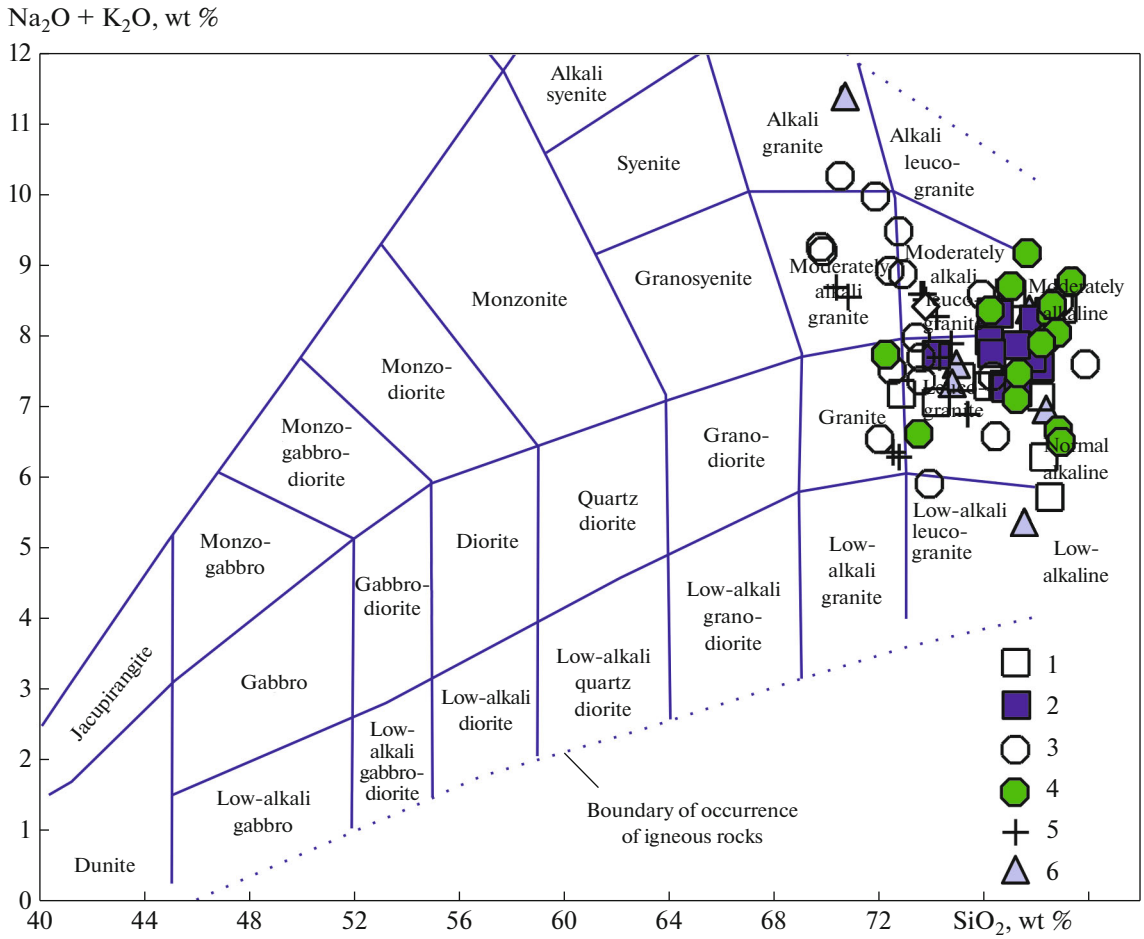

Fig. 2. TAS diagram for rocks of the Vodorazdelny pluton and its possible analogs after (Sharpenok et al., 2013). Granites from plutons: (1) Vangyr; (2) Kozhim; (3, 4) Mankhambo: (3) phase I; (4) phase II; (5) Vodorazdelny; (6) rhyolites of the Mount Sablya complex.

Moroin (Upper Riphean), and Mount Sablya (Sablegorsky) (Upper Riphean–Vendian) formation in the present-day edition of maps (Dushin et al., 2017). Blastomylonites and tectonic breccias of rocks of the frame in the granitoid "matrix" occur at the contact zone. The halos of hornfels and skarns are registered in the north, south, and east of the pluton.

The eastern part of the pluton is overlapped by boulder rocks with abundant coarse-grained porphyritic granites. In comparison with the southern part, no quartz porphyries and small-grained granites are found in the northern part of the pluton. The southern part has a lower thickness in comparison with the others, which is related to the occurrence of latitudinal faults and tectonic displacement. The granitoids of the pluton are cut by thin dikes of aplites.

The main volume of the Vodorazdelny pluton (main phase) includes the hypabyssal biotite granites. These are light grayish pinkish medium- to coarse-grained porphyritic rocks with K-feldspar phenocrysts ~1 cm in size. They are composed of microcline-perthite, plagioclase, quartz, biotite, and locally hornblende. The accessory minerals are allanite, titanite, and zircon; the secondary minerals are muscovite, chlorite, albite, and sericite. The rocks at the contacts of the pluton are characterized by a small-grained structure, the replacement of biotite with muscovite, the formation of magnetite, tourmaline, and rare garnet, and an increasing amount of quartz. The peripheral part of the pluton contains the light grayish pinkish small-grained porphyritic leucogranites, which transit to porphyry granites and together form zones up to 30–300 m thick. The leucogranites have a variable composition: quartz + albite + biotite, locally, with relics of more calcic plagioclase, which is replaced by albite along the rims. The relatively coarse-grained leucogranites contain microcline-perthite. Chervyakovskiy et al. (1992) indicated that the final stage of alteration is related to the formation of K-feldspar.

The quartz porphyries and porphyry granites are the shallowest rock types, which differ only in the degree of crystallization of the matrix. The phenocrysts include quartz and rare albite–oligoclase. The rock matrix is composed of microlites of quartz, plagioclase, and sericite, and accessory minerals include titanite, zircon, and magnetite.

MATERIALS AND METHODS

All analytical procedures were conducted at the Center for Collective Use "Geoanalitik" of the Institute of Geology and Geochemistry, Ural Branch, Russian Academy of Sciences (IGG UB RAS, Yekaterinburg, Russia). The contents of major oxides were measured on SRM-18 and EDX-900 HS spectrometers. The Fe_2O_3 and Na_2O contents were analyzed using X-ray fluorescence; the FeO and Na_2O contents and losses on ignition (LOI) were determined using classical chemical methods. The contents of trace elements were analyzed with the use of argon on an ELAN-9000 (PerkinElmer) quadrupole inductively coupled plasma mass spectrometer (ICP-MS). The analytical error is 0.1–1.0 rel. % (for different contents of elements).

The zircon grains were sampled from porphyritic biotite microcline granite of the main phase (Sample B-10, Tables 1, 2). The zircons were extracted from concentrates using heavy liquids, manually selected under a binocular microscope, emplaced into epoxy resin, and polished up to 1/2 thickness of the grains. Before the analyses, the polished sections were cleaned with ethanol and HNO_3 (3%).

The content of trace elements in zircons was analyzed on a NexION 300S ICP-MS (PerkinElmer) equipped with a NWR laser ablation system. The analytical method is described in (Chervyakovskaya et al., 2022). The analytical conditions included a crater diameter of 25 μm, a frequency of pulse repetition of 10 Hz, and an energy density of 10.5–11.5 J/cm^2. The results were processed in the GLITTER V4.4 program using an internal SiO_2 standard and NIST SRM 610 and NIST SRM 612 standard glasses as external primary and secondary standards, respectively. The analyses were conducted in terms of 10–12 measurements. The measurement error for NIST 610 and NIST 612 for the measured elements was 3–20% (1σ) and 3–25% (1σ), respectively.

The Lu–Hf isotopic system was studied on a Neptune Plus multicollector mass spectrometer (Thermo Fisher Scientific) equipped with a NWR 213 laser ablation system. The analytical method is described in (Chervyakovskaya et al., 2021). The analytical conditions included a crater diameter of 25 μm, a frequency of pulse repetition of 10 Hz, and an energy density of 11.5–12.5 J/cm^2. Zircon GJ-1 was used as a primary standard; zircons 91500, Plesovice, and Mud Tank were secondary standards; the procedure used a range of five measurements. The average weighted $^{176}Hf/^{177}Hf$ ratio for the GJ-1 and Mud Tank standards was 0.282042 ± 0.000017 (N = 8; ±2σ) and 0.282496 ± 0.000020 (N = 4; ±2σ), respectively. The values of a single measurement of the $^{176}Hf/^{177}Hf$ isotopic ratio for the 91500 and Plesovice standards were 0.282465 ± 0.000030 (±2σ) and 0.282300 ± 0.000053 (±2σ) within this session. The measurement error (2σ) of the $^{176}Hf/^{177}Hf$ isotopic ratio for the zircon standards was 0.011–0.020%.

The U–Pb age of zircons was analyzed on the NexION 300S ICP MS (PerkinElmer) equipped with a NWR 213 (ESI) laser ablation system. The analytical procedure and age calculation algorithm are described in (Zaitseva et al., 2016). The analytical conditions included a crater diameter of 25 μm, a frequency of pulse repetition of 10 Hz, and an energy density of 10–11 J/cm^2. The results were processed in the GLITTER V4.4 program. The primary standard zircon GJ-1 (secondary standards were zircons 91500 and Plesovice) was measured after ten unknowns. The U–Pb age of the GJ-1, 91500, and Plesovice zircons was 600.5 ± 1.9 Ma (N = 24; MSWD = 0.17; 1σ), 1065 ± 11 Ma (N = 4; MSWD = 0.001; 1σ), and 338 ± Ma (N = 6; MSWD = 0.014; 1σ), respectively, within this analytical session. The analytical error of the $^{206}Pb/^{238}U$ and $^{207}Pb/^{235}U$ isotopic ratios for the standards was 1.3–2.6% and 2.7–5.3% (1σ), respectively. The analysts were M.V. Chervyakovskaya and V.S. Chervyakovskiy.

PETROCHEMICAL FEATURES OF GRANITOIDS OF THE VODORAZDELNY PLUTON AS A KEY TO GEODYNAMIC INTERPRETATIONS

The chemical composition of granitoid samples of the Vodorazdelny pluton (Table 1) and their position on the TAS diagram (Sharpenok et al., 2013) show that the rocks correspond to moderately alkali granites and leucogranites (Fig. 2). They are calc-alkaline, subalkaline, and peraluminous. Most granites are high-K and some compositions correspond to medium-K types. The sum of alkalis of most samples is 7.6–8.7 wt %. The Na_2O/K_2O ratio of ~1 is shifted toward Na_2O in some altered samples. The rocks of the pluton are characterized by lower CaO, TiO_2, Al_2O_3, FeO*, and P_2O_5 contents at an increasing SiO_2 content, which is indicative of the differentiation of melt.

The K_2O and MgO contents are most variable, indicating weak postmagmatic alterations (K-feldspathization, albitization, chloritization) of some samples. The increasing role of accessory minerals in a balance of trace elements is responsible for the higher Nb, Ta, U, Hf, Y, and REE contents of rocks at increasing SiO_2 contents. The analysis of Ab–Q–Or cotectic shows that the rocks of the pluton formed at a pressure of 0.5–3.0 kbar.

The Rb content of most samples is 200–280 ppm, decreasing to 113 ppm in albitized Na_2O-rich varieties. The Sr content is 30–58 ppm, increasing to 150 ppm in varieties with the most calcic plagioclase. On the basis of the highest contents of these elements, the rocks of the Vodorazdelny pluton can be ascribed to an adamellite–granite type after Fershtater (1987).

The compositions of granites of the pluton in a QPMN field on the Rb–Sr diagram (Fershtater, 1987) correspond to those of the derivatives of continental

Table 1. Content of major oxides (wt %) and trace elements (ppm) in granitoids of the Vodorazdelny pluton

Components	Sample numbers													
	B-3	B-8	B-7	B-20	B-26	B-23	B-22	B-28	B-9	B-27	B-2	B-10	B-21	B-11
SiO_2	65.21	70.16	70.6	72.29	72.51	73.33	73.44	73.5	73.51	73.92	74.02	74.46	75.07	76
TiO_2	0.38	0.32	0.33	0.16	0.16	0.11	0.14	0.09	0.11	0.15	0.11	0.15	0.11	0.09
Al_2O_3	11.17	14.99	14.85	14.35	13.76	13.96	13.2	14.11	13.63	13.08	13.32	12.86	13.12	13.23
Fe_2O_3	1.80	1.86	1.06	1.12	1.07	1.28	1.2	1.73	1.43	1.11	1.09	1.32	1.47	0.70
FeO	0.74	0.91	1.63	1.09	1.09	0.73	0.91	0.36	0.64	1.09	0.91	1.18	0.54	0.43
MnO	0.04	0.05	0.06	0.06	0.06	0.05	0.04	0.02	0.03	0.04	0.05	0.04	0.03	0.04
MgO	7.13	0.83	0.86	1.45	1.27	0.28	0.39	0.37	0.39	0.34	0.46	0.35	0.44	0.06
CaO	5.93	1.54	1.6	1.18	1.21	0.68	0.58	0.59	0.7	0.64	0.74	0.73	0.88	0.69
Na_2O	2.32	4.19	4.39	4.19	4.19	4.31	3.94	4.19	4.06	3.97	4.19	3.45	5.62	3.66
K_2O	3.69	4.47	4.14	2.13	2.06	4.26	4.63	4.19	4.43	4.28	3.48	4.41	1.24	4.10
P_2O_5	0.08	0.12	0.12	0.09	0.09	0.07	0.0.8	0.08	0.07	0.08	0.07	0.08	0.07	0.01
LOI	1.38	0.74	1.39	1.91	1.91	0.6	0.61	0.82	0.67	0.56	0.63	0.55	1.02	0.67
Li	10.0	n.a.	n.a.	16.0	n.a.	13.0	n.a.	n.a.	14.0	n.a.	15.0	13.0	32.0	40.0
Be	0.9	4.0	3.5	5.1	4.5	2.8	3.8	7.7	3.6	7.3	3.3	3.1	4.6	3.0
Sc	7.0	5.0	5.0	7.0	8.0	4.4	7.0	6.0	7.0	8.0	6.0	6.0	7.5	5.0
V	40.0	22.0	9.0	6.5	9.0	6.5	7.0	0.0	8.0	15.0	7.5	7.5	6.5	3.1
Cr	40.0	n.a.	n.a.	0.8	n.a.	9.0	n.a.	n.a.	0.9	n.a.	1.1	1.0	0.9	0.9
Co	6.0	5.0	4.0	1.5	5.0	1.1	2.0	3.0	2.5	3.0	5.0	2.0	2.0	0.9
Ni	20.0	10.0	19.0	8.5	9.0	5.5	8.0	3.0	6.5	8.0	19.5	10.6	5.9	1.6
Cu	13.4	n.a.	n.a.	9.0	n.a.	6.0	n.a.	n.a.	4.1	n.a.	4.1	5.0	11.9	3.4
Zn	60.0	n.a.	n.a.	14.0	n.a.	30.0	n.a.	n.a.	30.0	n.a.	30.0	30.0	30.0	30.0
Ga	14.0	n.a.	n.a.	22.0	n.a.	19.0	n.a.	n.a.	21.0	n.a.	21.0	21.0	22.0	22.0
As	5.3	n.a.	n.a.	7.5	n.a.	5.8	n.a.	n.a.	6.0	n.a.	4.4	6.4	4.6	7.7
Se	0.6	n.a.	n.a.	0.9	n.a.	0.4	n.a.	n.a.	0.6	n.a.	0.7	0.7	1.1	1.1
Rb	90.0	217.0	225.0	118.0	115.0	221.0	288.0	160.0	216.0	228.0	113.5	186.0	200.5	240.0
Sr	270.0	152.0	136.0	47.0	31.0	40.0	57.0	13.0	55.0	46.0	55.0	58.0	45.5	40.0
Y	17.0	32.0	29.0	58.5	20.0	25.0	72.0	28.0	27.5	21.0	25.0	28.0	56.0	50.0
Zr	95.0	139.0	151.0	96.0	129.0	91.5	73.0	99.0	131.5	260.0	120.0	115.0	77.0	70.0
Nb	8.0	11.0	18.0	16.5	12.0	14.0	9.0	50.0	13.5	10.0	11.5	13.5	22.0	29.0
Mo	0.3	n.a.	n.a.	0.1	n.a.	0.1	n.a.	n.a.	0.3	n.a.	0.2	0.1	1.2	0.2
Cs	1.1	n.a.	n.a.	5.2	n.a.	2.7	n.a.	n.a.	3.1	n.a.	4.9	2.4	6.0	7.7
Ba	800.0	n.a.	n.a.	60.0	n.a.	170.0	n.a.	n.a.	120.0	n.a.	130.0	130.0	140.0	80.0
La	22.0	n.a.	n.a.	15.0	n.a.	12.0	n.a.	n.a.	28.0	n.a.	27.0	15.0	16.0	10.0
Ce	44.0	n.a.	n.a.	37.0	n.a.	32.0	n.a.	n.a.	70.0	n.a.	60.0	50.0	39.0	29.0
Pr	5.4	n.a.	n.a.	4.0	n.a.	3.7	n.a.	n.a.	7.0	n.a.	7.0	4.0	5.0	3.1
Nd	20.0	n.a.	n.a.	17.0	n.a.	13.0	n.a.	n.a.	26.0	n.a.	24.0	16.0	18.0	12.0
Sm	4.1	n.a.	n.a.	5.0	n.a.	3.1	n.a.	n.a.	6.0	n.a.	5.0	4.1	6.0	4.4
Eu	1.1	n.a.	n.a.	0.2	n.a.	0.2	n.a.	n.a.	0.4	n.a.	0.4	0.4	0.3	0.3
Gd	4.0	n.a.	n.a.	7.0	n.a.	3.1	n.a.	n.a.	5.0	n.a.	5.0	4.0	7.0	6.0
Tb	0.6	n.a.	n.a.	1.2	n.a.	0.5	n.a.	n.a.	0.8	n.a.	0.8	0.7	1.3	1.3
Dy	3.3	n.a.	n.a.	8.0	n.a.	2.9	n.a.	n.a.	4.6	n.a.	5.0	5.0	9.0	9.0
Ho	0.7	n.a.	n.a.	1.7	n.a.	0.6	n.a.	n.a.	0.9	n.a.	0.9	1.0	1.8	2.0
Er	2.0	n.a.	n.a.	5.0	n.a.	1.6	n.a.	n.a.	2.7	n.a.	2.8	2.9	5.0	6.0

Table 1. (Contd.)

Components	Sample numbers													
	B-3	B-8	B-7	B-20	B-26	B-23	B-22	B-28	B-9	B-27	B-2	B-10	B-21	B-11
Tm	0.3	n.a.	n.a.	0.8	n.a.	0.3	n.a.	n.a.	0.4	n.a.	0.4	0.5	0.8	0.9
Yb	1.9	n.a.	n.a.	5.0	n.a.	1.7	n.a.	n.a.	2.8	n.a.	2.8	3.1	5.0	6.0
Lu	0.3	n.a.	n.a.	0.8	n.a.	0.2	n.a.	n.a.	0.4	n.a.	0.4	0.5	0.8	0.8
Hf	2.9	n.a.	n.a.	4.0	n.a.	3.0	n.a.	n.a.	4.0	n.a.	3.0	4.0	4.0	3.0
Ta	0.6	n.a.	n.a.	2.7	n.a.	2.3	n.a.	n.a.	1.7	n.a.	1.4	1.8	2.8	1.6
W	0.7	n.a.	n.a.	0.4	n.a.	0.6	n.a.	n.a.	0.3	n.a.	0.3	0.3	0.6	0.5
Pb	3.0	n.a.	n.a.	2.5	n.a.	15.0	n.a.	n.a.	14.0	n.a.	16.0	14.0	10.0	24.0
Th	6.0	n.a.	n.a.	19.8	n.a.	7.0	n.a.	n.a.	25.8	n.a.	24.0	20.7	23.1	21.8
U	1.5	n.a.	n.a.	4.0	n.a.	1.7	n.a.	n.a.	3.4	n.a.	4.0	3.6	4.2	5.0

n.a., not analyzed.

and island-arc tholeiitic magmas. On a series of diagrams (Fig. 3), the composition matches that of the I-type (rather than A-type) granites.

In addition to the compositions of granites of the Vodorazdelny pluton, we plotted the compositions of the nearby Vangyr and Kozhim intrusions of the Salner–Mankhambo complex on the Pearce diagram, which characterizes the geodynamic settings (Fig. 4). The compositions of granites of the Vodorazdelny pluton lie at the boundaries of the VAG–WPG–Syn-COLG fields.

The total REE content of granites of the Vodorazdelny pluton are 90–140 ppm; the chondrite-normalized REE patterns are weakly differentiated (the La/Yb ratio is 2–10) and contain a strong negative Eu anomaly (Fig. 5a). Note that the absence of Eu anomaly is one of the typical features of early orogenic Carboniferous granites of the Uralian Orogen located eastward of the Main Uralian Fault Zone (Fershtater, 2013). The earlier (Ordovician–Silurian) supra-subduction rocks exhibit a negative Eu anomaly (Petrov et al., 2017). This anomaly is observed almost in all Late Riphean–Vendian–Cambrian granitoids of the Subpolar Urals irrespective of their geodynamic setting (Udoratina et al., 2021). The N-MORB-normalized compositions of the studied granites exhibit negative Nb, Ti, and Zr anomalies typical of supra-subduction rocks (Fig. 5b). On the other hand, they are similar to an average composition of the upper continental crust. This dual behavior can indicate a heterogeneous substrate.

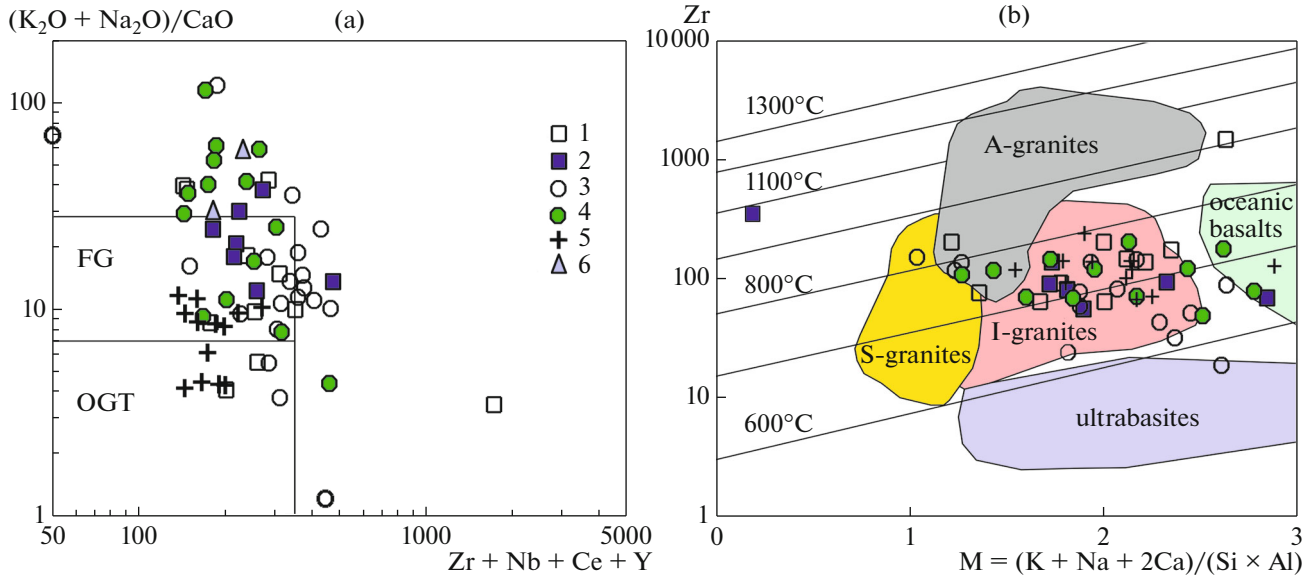

Fig. 3. Whalen diagram (Whalen et al., 1979) (a) for various types of granites and correlation between Zr content of rocks and crystallization temperature (b) after (Hanchar and Watson, 2003; Kostitsyn et al., 2015). FG, fractionated granite; OGT, non-fractionated I-, S-, and M-type granites. For legend, see Fig. 2.

Table 2. Content of trace elements (ppm) and indicator ratios of zircons of the Vodorazdelny pluton

Number/ element	88	90	90_2	91	95	96	97	100	113	114	115
Sc	351	351	368	297	370	337	262	406	390	474	428
Ti	11.9	34.9	44.7	12.5	11.5	79.7	13.9	40.6	14.7	70.0	34.5
Y	1338	1947	1882	1201	1527	7999	1443	2841	4105	1530	1086
Nb	1.79	1.97	1.10	1.26	5.2	4.31	15.9	3.87	2.22	7.72	5.44
Hf	12557	12284	13062	11330	11216	9919	14084	13180	15165	16049	13852
Ta	0.27	1.43	1.45	0.77	0.35	1.32	5.92	0.83	1.36	2.36	n/d
Pb	31.2	37.6	38.9	29.1	50.0	82.2	147	64.4	74.9	53.5	63.9
Th	46	85	92	53	75	186	95	137	156	85.9	56.9
U	79.7	91.5	101	68.4	98.9	161	202	150	169	128	139
La	0.088	1.94	0.010	0.165	0.010	271	3.32	0.130	0.220	0.010	2.4
Ce	3.13	9.45	5.75	4.13	5.20	588	17.4	7.71	8.82	6.49	5.63
Pr	0.137	0.980	0.114	0.290	0.310	75.5	1.48	0.410	0.170	0.160	0.460
Nd	0.440	6.90	1.84	0.93	0.85	369	7.10	1.34	5.47	2.08	6.04
Sm	2.94	9.56	7.35	2.06	1.89	169	7.36	8.91	18.2	2.30	8.93
Eu	0.870	0.650	1.04	0.260	0.480	29.5	0.320	0.670	3.09	0.290	1.14
Gd	29.1	38.8	39.2	37.8	18.7	625	40.7	62.6	97.8	26.2	36.0
Tb	9.04	11.0	13.2	5.94	7.58	157	10.1	18.1	30.5	9.41	8.94
Dy	116	170	191	104	142	1275	154	244	386	114	94
Ho	48.5	59.0	73.2	40.8	53.4	330	53.5	82.7	150	48.3	50.5
Er	197	298	294	195	267	955	241	426	584	228	180
Tm	44.3	56.7	66.0	45.6	47.3	198	47.8	79.4	114	48.3	45.4
Yb	387	508	563	384	473	1355	412	650	964	440	477
Lu	73.4	91.0	92.5	76.1	88.9	236	75.9	131.4	205.6	80.5	74.5
Age	–	–	–	–	543	–	1599	–	–	552	–
REE t	911	1262	1347	896	1106	6633	1071	1714	2567	1006	990
Zr/Hf	53.0	58.7	57.6	51.9	67.5	66.3	51.7	59.9	58.2	54.9	65.1
Th/U	0.580	0.920	0.920	0.770	0.750	1.160	0.470	0.910	0.920	0.670	0.410
U/Yb	0.206	0.180	0.179	0.178	0.209	0.119	0.490	0.231	0.175	0.291	0.290
Yb/Sm	132	53.2	76.6	187	250	8.02	55.9	73.0	53.0	191	53.4
Eu/Eu*	0.290	0.100	0.190	0.090	0.250	0.280	0.060	0.090	0.220	0.110	0.190
Ce/Ce*	6.86	1.65	41.0	4.62	22.7	0.990	1.88	8.04	11.0	39.1	1.31
$(Sm/La)_n$	53.1	7.83	1167	19.8	300	0.990	3.52	109	131	365	5.9

Table 2. (Contd.)

Number/ element	116	117	120	121	134	135	136	138	139	143	145	146
Sc	444	458	470	440	534	431	390	435	399	447	414	376
Ti	22.0	n.d.	n.d.	15.0	34.4	n.d.	n.d.	12.68	16.77	n.d.	98.4	6.57
Y	1981	3068	1482	1494	4554	2633	1210	1854	1924	1703	2384	3875
Nb	1.81	5.46	2.98	4.58	1.48	3.18	3.35	0.760	1.74	3.77	1.90	2.64
Hf	15286	15934	11833	13370	9955	14666	13385	12556	12619	12633	12361	14493
Ta	1.35	1.67	0.360	0.84	0.760	2.87	1.38	0.390	0.430	1.15	0.930	1.41
Pb	45.0	75.2	31.5	40.1	40.4	73.3	55.5	33.3	34.3	38.0	44.3	105
Th	97.0	163	51.1	56.3	119	157	76.2	71.7	68.0	65.6	78.0	134
U	122	176	69.4	72.0	99.5	191	121	69.4	87.0	90.3	107	272
La	2.97	0.960	0.010	0.010	0.580	5.58	0.010	0.010	0.010	0.085	0.500	0.010
Ce	13.4	12.3	2.46	3.27	4.32	25.4	8.77	2.23	4.64	3.81	6.28	8.51
Pr	1.15	0.530	0.320	0.330	0.450	2.47	0.390	0.116	0.128	0.066	0.520	0.150
Nd	9.80	4.04	3.08	2.71	10.2	16.7	0.830	3.39	2.49	1.72	7.30	1.95
Sm	9.18	8.06	1.95	3.01	29.9	12.6	3.23	7.51	7.82	2.85	6.85	5.41
Eu	1.18	0.910	0.500	n/d	7.21	1.50	0.240	1.49	0.590	0.480	0.790	0.550
Gd	31.9	61.1	28.6	24.2	144	63.6	25.4	43.74	44.16	28.60	40.17	47.57
Tb	9.86	24.8	10.7	11.6	36.2	23.5	6.66	13.10	12.96	9.83	15.36	19.75
Dy	160	261	130	146	534	265	110	162	163	157	231	331
Ho	64.6	113.5	51.1	46.4	181.4	102.4	44.5	67.8	63.6	59.3	79.7	125
Er	312	455	227	221	627	417	193	258	274	251	351	599
Tm	64.3	99.2	48.0	51.9	127	80.6	39.3	59.0	55.3	53.2	73.1	104
Yb	566	845	433	388	1028	691	355	461	491	444	683	956
Lu	116	165	90.2	86.4	184	131	67.3	96.7	91.7	93.3	116	196
Age	852	525	560	–	615	551	523	573	608	–	–	530
REE t	1362	2050	1027	985	2914	1838	855	1176	1212	1106	1613	2394
Zr/Hf	55.2	56.3	69.4	57.7	83.5	51.4	56.8	64.6	65.8	62.7	62.1	53.3
Th/U	0.790	0.930	0.740	0.780	1.190	0.820	0.630	1.03	0.780	0.730	0.730	0.490
U/Yb	0.216	0.208	0.160	0.185	0.097	0.277	0.341	0.151	0.177	0.203	0.157	0.285
Yb/Sm	61.6	105	222	129	34	54.8	110	61.4	62.8	156	99.8	177
Eu/Eu*	0.210	0.130	0.200	n/d	0.340	0.160	0.080	0.250	0.100	0.160	0.150	0.100
Ce/Ce*	1.75	4.23	10.6	14.0	2.04	1.65	34.3	15.8	31.2	12.2	3.0	52.9
$(Sm/La)_n$	4.9	13.3	310	478	82.0	3.59	513	1193	1242	53.3	21.8	859

Age in the first column means the $^{238}U–^{206}Pb$ age of zircons (Ma); n.d., not determined; dash, not analyzed.

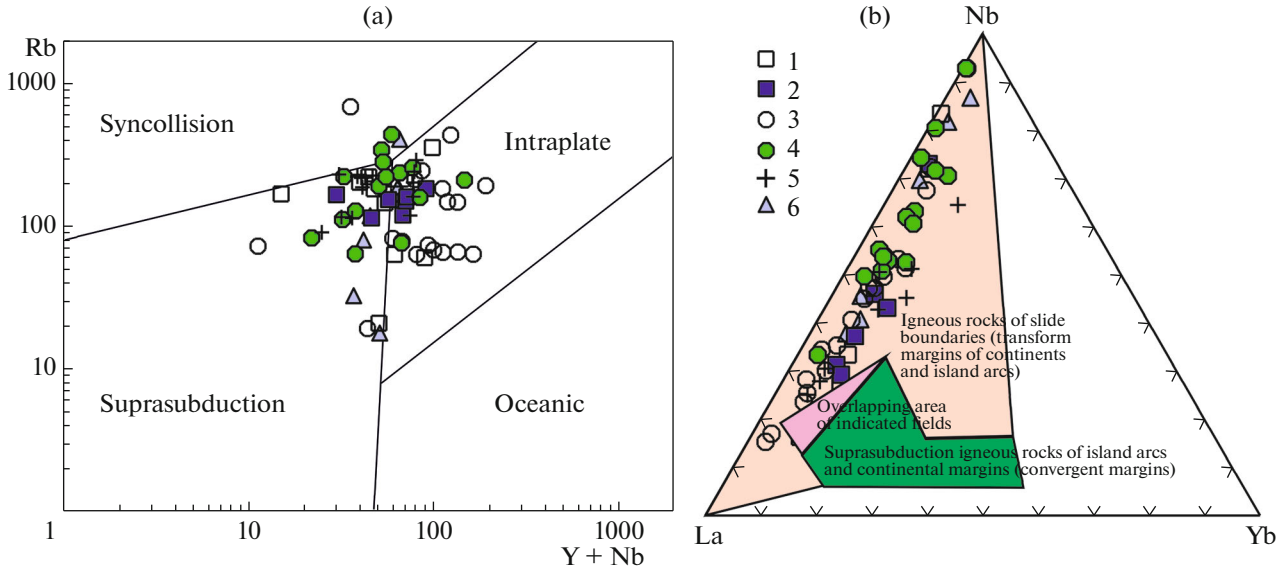

Fig. 4. Pearce diagram (Pearce et al., 1984) of geodynamic settings of the formation of granitoids. For legend, see Fig. 2.

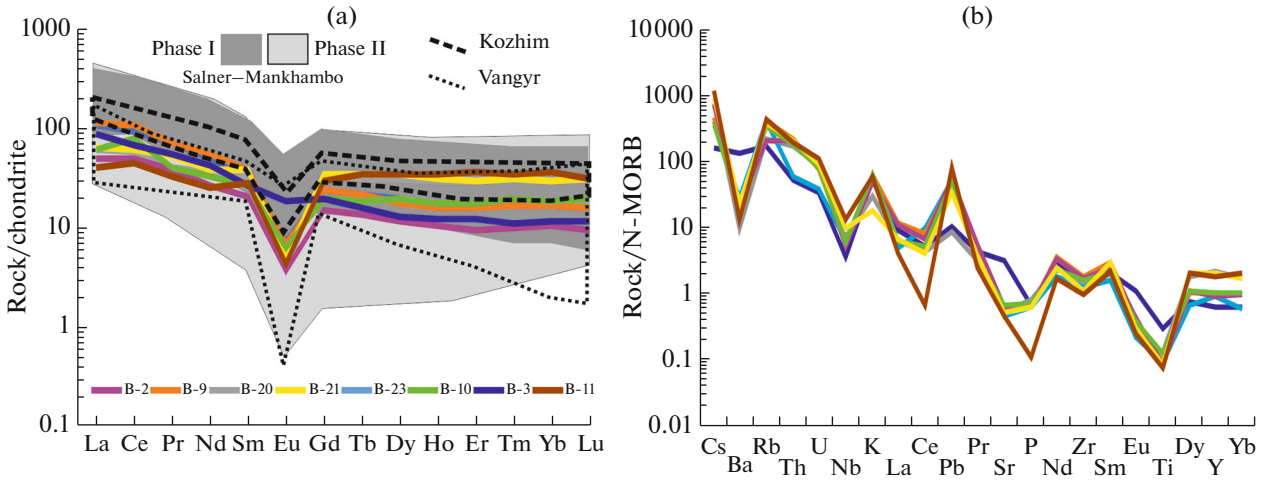

Fig. 5. Chondrite-normalized (a) and N-MORB-normalized (b) (McDonough and Sun, 1995) trace element pattern in a series of granitoids of the Lyapin Anticlinorium. Sample numbers correspond to those in Table 2. The average composition of the upper continental crust is shown after (Rudnik and Gao, 2003).

A complex of parameters thus indicates the suprasubduction setting of the formation of granites of the Vodorazdelny pluton. To refine this conclusion, we determined their age and isotopic parameters on the basis of the analysis of the chemical composition (identification of a genetic nature), age, and study of the Lu–Hf system of zircons from granite of the main phase of the pluton.

MORPHOLOGY, CHEMICAL COMPOSITION, AND GENETIC FEATURES OF ZIRCONS

The photomicrographs of zircon grains are shown in Fig. 6. They are semitransparent or muddy, pinkish or brownish pinkish; most zircons are detrital forms unfavorable for the identification of their morphological types. Pystina and Pystin (2017) recently described the typical morphological features of zircons and recognized various crystal types in granitoids of the Subpolar Urals of various ages: Nikolaishor (Early Proterozoic), Kozhim (Middle–Upper Riphean), and Mankhambo (Early Cambrian) complexes. We tried to relate the features of our grains to characteristics published in this work.

The most intact zircon grains of the Vodorazdelny pluton are conditionally divided into two types on the basis of their optical and CL images. Type 1 includes semitransparent pale euhedral crystals with an elongation coefficient of 4–5, the edges (100), (110), and (113),

and weakly corroded outer surface with mostly transverse fractures. In the CL regime, these grains have concentric growth zonation (intercalation of fine light and dark bands of various widths); they locally contain inclusions and unaltered irregular cores. In some cases, the zonal grains are rimmed by light regeneration rims or contain ancient cores. This is a so-called torpedo-like type after Pystina and Pystin (2017). Type 2 grains are more muddy, brownish of irregular form, wider in sections (the elongation coefficient is no more 1.5) with a network of variously oriented locally gradual fractures, strongly corroded surface with caverns, and possible edges (110), (111), and (321). The relation between the relative areas of the prism and pyramid indicates a predominance of a prismatic belt. In CL images, these grains often have a dark core domain, locally, chopped; the intermediate zones are irregularly spotty (light–dark), locally, with sectoriality. Some areas exhibit fine zonation. The rims are mostly corroded and some grains are overgrown with new lighter material. This is the "zircon" type of grains. Some large fragments can be ascribed to the "zirtolite" type. A similar assemblage of morphological types shown in (Pystina and Pystin, 2017) is typical of shallow granites of the Kozhim pluton. Unfortunately, the variations in U and Th contents were not analyzed in various zones of single crystals. The primary shape and structure of many zircons from granites of the Vodorazdelny pluton are disturbed by multiple tectono-thermal processes.

The contents of trace elements in zircons from the Vodorazdelny granites are shown in Table 2. Owing to the beam size of 25 μm, some analyses with high Ti, Th, and Ca contents are excluded, because they indicate the presence of mineral inclusions. In total, about 25 analyses of zircons were conducted.

It is traditionally considered that U and Th behavior in zircons may be informative of their genesis. The U and Th contents of our zircons are relatively low: 60–270 ppm U and 46–190 ppm Th. Some points yield almost a linear direct U–Th correlation, indicating a common origin of the population of grains; some measurements strong deviate from a general correlation. The Th/U ratios for all grains are 0.41–1.20 (0.7–0.9 for most grains).

The Zr/Hf ratio of our granites is 50–67, locally reaching 80. The Ti content of most zircon grains is <15 ppm (locally, 70–98 ppm). This indicates the different degree of alteration, structural disordering, and/or zircon genesis (magmatic or hydrothermal). The higher Ti contents of zircons can be affected not only by microinclusions. Harrison and Schmitt (2007) showed that Ti in zircons can be absorbed by micropores or fractures, especially in areas with intense structural disordering and hydration. The Ti activity is accepted by us as 1 owing to uncertain paragenetic relations of zircon to Ti minerals. Thus, the temperatures are the minimum possible. The calculated temperatures after (Ferry and Watson, 2007) for the grains with significant but lower Ti contents are 707–790°C, which is consistent with the calculations for rocks (Fig. 3b).

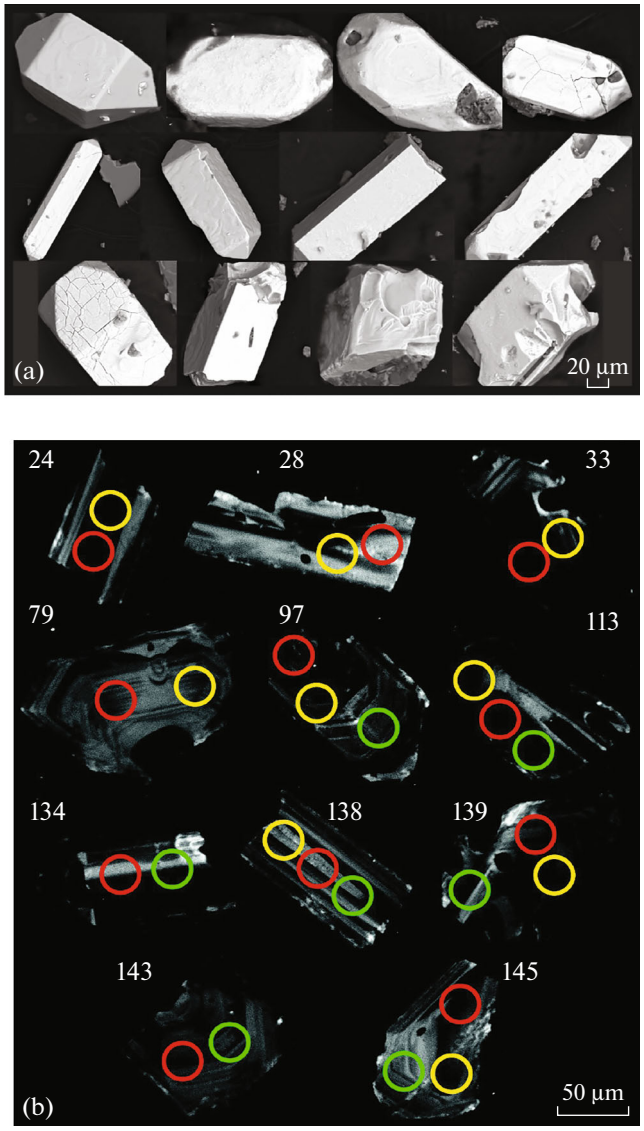

Fig. 6. Optical photomicrographs (a) of typical zircons from granites of the Vodorazdelny pluton and CL images (b) of zircons grains analyzed for U–Pb age. Circles indicate the analytical points of U–Pb age (gray), Lu and Hf isotopes (white), and trace element composition (black). Sample numbers correspond to those in Tables 3 and 4.

The contents of other HFSEs of our zircons are variable (ppm): 1086–7999 Y, 0.76–15 Nb, 0.27–6 Ta, and 12600–14500 Hf (Table 2). The REEs in rocks and igneous minerals are considered to be unaffected by superimposed processes. The total REE content of zircons is 850–6600 ppm and the total light REE (LREE) content is 7–1472 ppm. The values of index ratios (Fig. 7) also vary significantly.

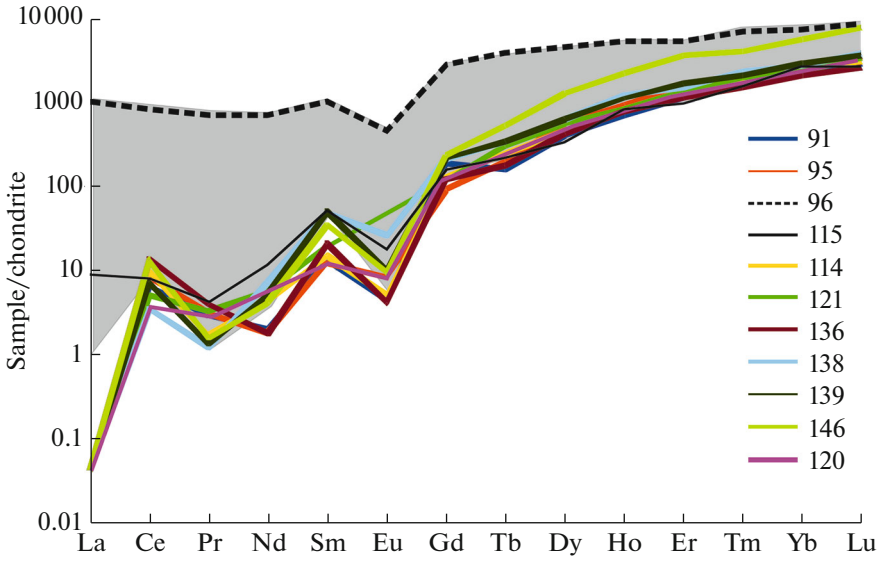

Fig. 7. Chondrite-normalized (McDonough and Sun, 1995) REE patterns of zircons from granites of the Vodorazdelny pluton. The area of hydrothermal zircons compositions shows by gray field.

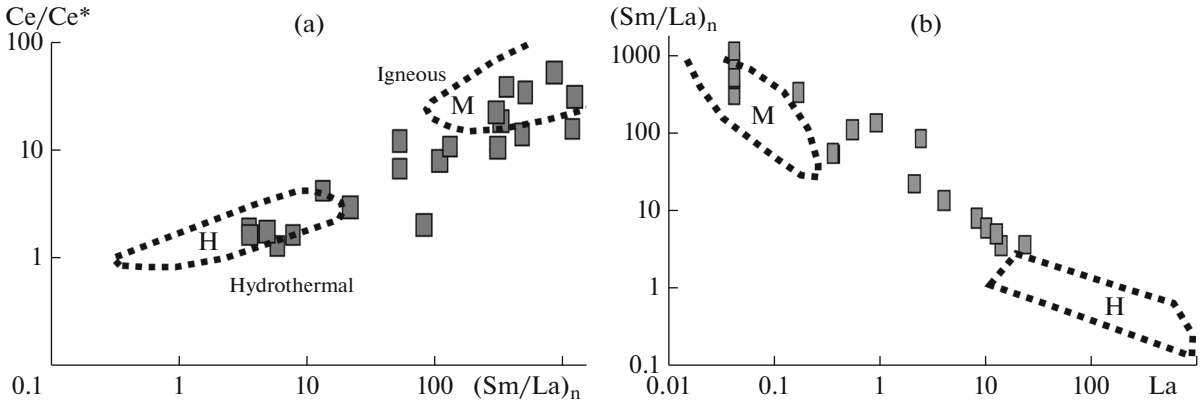

Fig. 8. Hoskin (2005) diagrams of zircon genesis.

According to the published data, the Th/U ratio of most igneous zircons is 0.3–0.7; the lower values (0.3–0.1) indicate the growth from a fluid phase (Rubatto, 2002; Hoskin and Schaltegger, 2003; Fu et al., 2009; Zhong et al., 2018). The low Th/U ratio often indicates the degree of structural disordering and the peculiarities of the composition of zircons and their host rocks rather than the genesis. The zircons of various origins (early, late, postmagmatic, metamorphic) exhibit a wide range of U and Th contents (Pelleter et al., 2007; Balashov and Skublov, 2011; Wang et al., 2013). The Th/U value of our zircons is >0.4; however, the morphology and structure of many grains indicate a strong change in the structure and evidently the composition. Nonetheless, many grains preserve primary geochemical characteristics.

For conclusions on the nature of zircons, we used the diagrams of Hoskin (2005) and Fu et al. (2009) (Fig. 8). The analysis of a current database of published and original data show that the field of igneous compositions (I) could be elongated downward. A significant part of the compositions of our zircons lies in this field and is further extended through the intermediate compositions to the field of "hydrothermal" (H) type and partly belongs to the latter. As a rule, the zircons from the same rock with increasing structural disordering, degree of alterations, or evolution of the composition of postmagmatic fluid phase exhibit a decreasing Ce/Ce* value, an increasing $(Sm/La)_n$ value, and a higher LREE content (the most contrasting being La) (Balashov and Skublov, 2011; Trail et al., 2012; Loucks et al., 2018). In our case, the La content and Ce/Ce* value also have a reverse correlation; some points with the highest La content (very high degree of disordering) make the correlation nonlinear.

In general, the zircon grains 91, 95, 100, 114, 120, 121, 136, 138, 139, and 146 are igneous on the basis of several parameters (Figs. 7, 8). Note that similar parameters do not mean their synchronous age. By

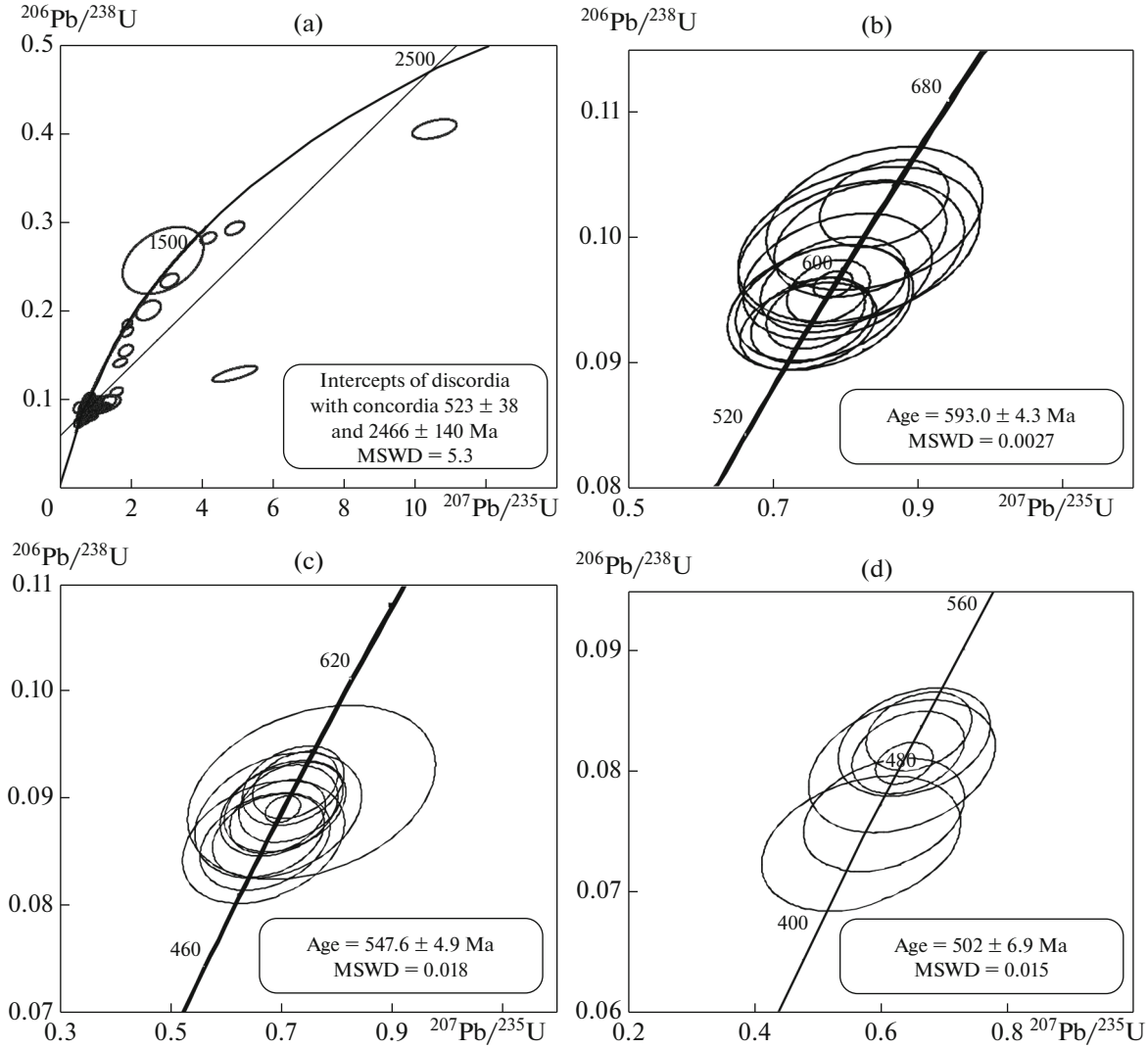

Fig. 9. U–Pb diagram with concordia (all grains) (a) and areas (b–d) corresponding to different age clusters in zircons from granites of the Vodorazdelny pluton.

outer and inner structure, the zircons also belong to different groups. The other zircons form trends with a significantly higher "light" branch of a pattern and smoothed Ce/Ce* value (this is evident from the Hoskin's diagrams; thus, the trends of zircons from the H field are shown as a field).

According to the diagram and criteria elaborated by Belousova et al. (2002), the compositions of zircons from granites of the Vodorazdelny pluton fall to the overlapping fields of derivative melts of granitic and syenitic composition.

U–Pb AGE OF ZIRCONS OF THE VODORAZDELNY PLUTON

The U–Pb age was determined for 119 zircon grains from granites of the Vodorazdelny pluton. The histogram of these ages is shown in Fig. 10. Many age values do not correspond to concordia (at a given MSWD on an agreement line) (Fig. 9). Many igneous grains show a high discordance, and thus they are excluded from consideration. The ancient (variously altered) cores have the ages of 2189, 1660, 1471, 1354, 1176–927, 852, and 780 Ma.

We also excluded the grains with high U and Th contents; 30 grains were selected with the discordance of <4% and consistent U and Th contents, which provide a direct correlation similar to linear. In our opinion (based on the geological evolution of magmatism of the Lyapin Anticlinorium), three age clusters can be distinguished among the measured ages (Table 3): (1) 502 ± 7 Ma, MSWD of 0.015, probability of 0.90; (2) 548 ± 5 Ma, MSWD of 0.018, probability of 0.89; (3) 593 ± 4 Ma, MSWD = 0.0027, probability of 0.96.

The ancient zircon grains (852, 927, and 1599 Ma) have distinct REE patterns (Fig. 9). The highest alteration is shown by grain 96; thus, its age is probably

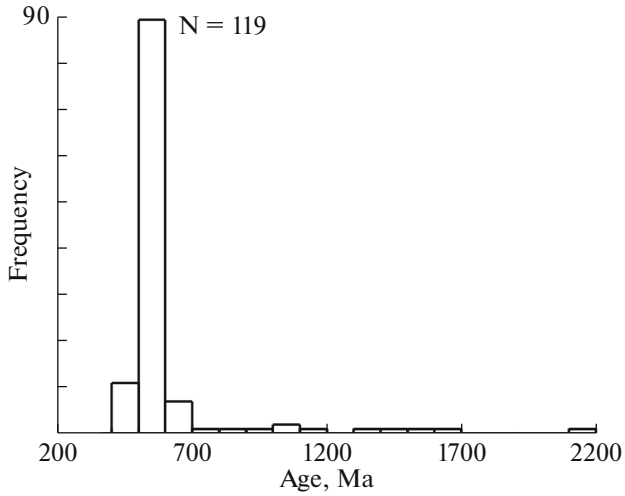

Fig. 10. Histogram of age distribution of zircons from granites of the Vodorazdelny pluton (all analyzed grains).

young. Grain 114 has a clear magmatic trend and grain 115 shows weak alteration.

Lu–Hf SYSTEM IN ZIRCONS OF GRANITES OF THE VODORAZDELNY PLUTON

The values of the primary ratios ($^{176}Hf/^{177}Hf$) and ε_{Hf} for selected grains are calculated for the age by the measured $^{207}/^{206}Pb$ ratio (Table 4, Fig. 11). The average $^{176}Hf/^{177}Hf$ and ε_{Hf} values were calculated for the $^{238}U–^{206}Pb$ age from Tables 2 and 3. As seen from the previous section, our zircons belong to at least three age clusters, which probably differ in origin and/or the degree of alteration. On the basis of the outer and inner structure and ages, the zircons are conditionally subdivided into three groups by isotopic parameters. Group I includes the zircons of 2198, 1599, and 1354 Ma, as well as 632 and 612 Ma (because they are older than the main age population and most likely are a result of transformation of older varieties). These grains have a positive $\varepsilon_{Hf}(t)$ value of 0.8–13 (21??). Group II includes the igneous zircons of 608–573 Ma with a corresponding REE behavior (the composition was selectively analyzed); they are characterized by $\varepsilon_{Hf}(t)$ values close to 0 (from –1.1 to 1.4) excluding grain 77 with a high discordance. It has a spotty texture and a hourglass structure and is probably an alteration product of older zircon. Group III includes other grains with ages of 565–493 Ma mostly with negative $\varepsilon_{Hf}(t)$ values from –1 to –8, excluding grains 145 and 82 with weakly positive $\varepsilon_{Hf}(t)$ values.

The zircons from different groups are shown by different symbols in Fig. 11. Their greater part lies below a DM line, approaching CHUR, and slightly below the latter. In our opinion, we can discuss a decrease in $\varepsilon_{Hf}(t)$ values as the age of zircons becomes younger.

DISCUSSION

Age Relations of Granitic Plutons of the Kozhim Block and Evolution of Geodynamic Settings

As was shown above, the Kozhim, Vangyr, and Vodorazdelny plutons in latest editions of the 1 : 200000 State Geological Map (Ivanov et al., 2013b) are ascribed to the Vendian–Early Cambrian Salner–Mankhambo (phase II) Complex. Udoratina et al. (2020) mention that, in this interpretation, the age of the Kozhim granites "corresponds to riftogenic geodynamic settings (520–480 Ma), which were favorable

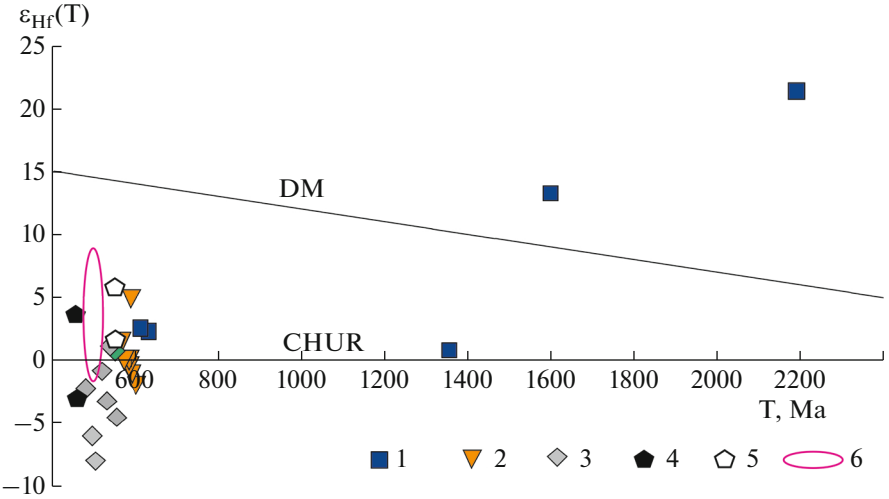

Fig. 11. Age–$\varepsilon_{Hf}(t)$ diagram for zircons of some plutons of the Subpolar Urals. Zircons from granites: (1–3) Vodorazdelny pluton: (1) ancient cores; (2) main population, the age of which characterizes the age of rocks; (3) young rims; (4–6) after published data on the (4) Kozhim and (5) Vangyr plutons and (6) Salner–Mankhambo Complex (Kuznetsov and Udoratina, 2007; Dushin et al., 2017; Udoratina et al., 2020, 2021).

Table 3. Results of isotopic analysis and age of zircons from granites of the Vodorazdelny pluton

No.	Content, μg/g			Isotope ratios						R, rel. units	Age, Ma				D, %
	Pb*	Th	U	$^{207}Pb/^{206}Pb$	±1σ	$^{207}Pb/^{235}U$	±1σ	$^{206}Pb/^{238}U$	±1σ		$^{207}Pb/^{235}U$	±1σ	$^{206}Pb/^{238}U$	±1σ	
2	41	74	109	0.0575	0.0049	0.648	0.058	0.0818	0.0023	0.32	507	36	507	14	0.00
8	62	87	147	0.0595	0.0063	0.774	0.086	0.0945	0.0034	0.32	582	49	582	20	0.00
11	68	104	173	0.0595	0.0049	0.732	0.063	0.0893	0.0025	0.32	558	37	552	15	1.08
14	56	123	166	0.0579	0.0075	0.610	0.083	0.0765	0.0032	0.31	484	52	475	19	1.86
15	54	101	141	0.0582	0.0055	0.710	0.071	0.0885	0.0028	0.32	545	42	547	17	–0.37
19	28	48	88	0.0563	0.0097	0.575	0.103	0.0740	0.0038	0.29	461	66	460	23	0.22
24	60	103	147	0.0595	0.0027	0.786	0.039	0.0958	0.0017	0.36	589	22	590	10	-0.17
28	46	75	105	0.0608	0.0040	0.864	0.060	0.1030	0.0024	0.33	632	32	632	14	0.00
33	83	146	206	0.0593	0.0033	0.768	0.046	0.0940	0.0019	0.35	579	26	579	11	0.00
39	48	82	111	0.0606	0.0068	0.851	0.100	0.1018	0.0039	0.32	625	55	625	23	0.00
43	53	63	139	0.0589	0.0057	0.722	0.074	0.0889	0.0028	0.31	552	43	549	17	0.54
51	37	64	97	0.0584	0.0079	0.709	0.101	0.0881	0.0039	0.31	544	60	544	23	0.00
57	61	118	165	0.0578	0.0079	0.682	0.098	0.0856	0.0038	0.31	528	59	529	23	–0.19
59	38	63	102	0.0582	0.0054	0.691	0.068	0.0862	0.0026	0.31	534	41	533	15	0.19
65	92	201	252	0.0577	0.0045	0.665	0.055	0.0837	0.0022	0.32	518	33	518	13	0.00
68	37	81	106	0.0574	0.0083	0.639	0.097	0.0807	0.0038	0.31	502	60	500	22	0.40
69	69	120	169	0.0592	0.0041	0.763	0.057	0.0934	0.0023	0.33	576	33	576	14	0.00
74	54	58	129	0.0595	0.0058	0.777	0.081	0.0949	0.0032	0.32	584	46	584	19	0.00
75	26	37	59	0.0603	0.0078	0.829	0.112	0.0997	0.0042	0.31	613	62	612	25	0.16
79	41	62	97	0.0597	0.0062	0.799	0.088	0.0970	0.0034	0.32	596	50	597	20	–0.17
90	60	135	143	0.0679	0.0056	0.873	0.077	0.0933	0.0028	0.34	637	42	575	16	9.73
95	76	190	196	0.0649	0.0049	0.786	0.063	0.0879	0.0024	0.33	589	36	543	14	7.81
113	88	210	220	0.0588	0.0046	0.737	0.061	0.0909	0.0025	0.32	561	36	561	15	0.00
123	68	172	176	0.0584	0.0045	0.708	0.058	0.0880	0.0023	0.32	543	34	543	14	0.00
124	26	44	71	0.0577	0.0066	0.658	0.079	0.0827	0.0031	0.31	513	48	512	18	0.19
133	36	105	95	0.0580	0.0064	0.684	0.079	0.0856	0.0030	0.31	529	47	530	18	–0.19
134	96	182	219	0.0603	0.0055	0.831	0.080	0.1000	0.0031	0.32	614	44	615	18	–0.16
138	30	61	74	0.0592	0.0047	0.758	0.063	0.0929	0.0024	0.31	573	37	573	14	0.00
139	29	42	68	0.0600	0.0073	0.818	0.105	0.0989	0.0039	0.31	607	59	608	23	–0.16
141	79	139	198	0.0591	0.0039	0.740	0.051	0.0909	0.0021	0.33	562	30	561	12	0.18
143	35	61	83	0.0597	0.0048	0.792	0.067	0.0963	0.0026	0.31	592	38	593	15	–0.17
148	35	52	82	0.0619	0.0115	0.770	0.150	0.0903	0.0054	0.31	580	86	557	32	3.97

No radiogenic lead was detected in the studied samples. $^{206}Pb^*$, the Pb content calculated by ^{206}Pb isotope. R, correlation coefficient of $^{207}Pb/^{235}U$–$^{206}Pb/^{238}U$ ratios. D, discordance.

Table 4. Results of analysis of Lu–Hf isotopic system and model age of zircons from granites of the Vodorazdelny pluton

No.	T, Ma	$^{176}Yb/^{177}Hf$	$^{176}Lu/^{177}Hf$	$^{176}Hf/^{177}Hf$	±2σ	$\varepsilon_{Hf}(t)$	T(DM), Ma	$T(DM)^C$, Ma	$^{176}Hf/^{177}Hf_t$
130	2189	0.02781	0.00085	0.282025	0.000093	21.4	1717	1418	0.281989
97	1599	0.04273	0.00101	0.282171	0.000051	13.3	1522	1474	0.282140
16	1354	0.03217	0.00076	0.281982	0.000050	0.8	1798	2080	0.281962
28	632	0.05977	0.00129	0.282455	0.000059	2.3	1129	1444	0.282440
75	612	0.03984	0.00094	0.282474	0.000078	2.6	1097	1403	0.282463
139	608	0.04106	0.00099	0.282352	0.000074	–2.1	1276	1699	0.282341
79	597	0.04384	0.00100	0.282389	0.000072	–1.1	1232	1634	0.282377
77	595	0.06072	0.00127	0.282541	0.000087	4.8	996	1251	0.282527
24	590	0.05887	0.00152	0.282391	0.000069	–0.6	1211	1602	0.282374
72	590	0.09273	0.00213	0.282405	0.000087	–0.04	1200	1586	0.282382
33	579	0.08599	0.00242	0.282432	0.000080	–0.04	1196	1586	0.282405
138	573	0.05208	0.00123	0.282480	0.000060	1.4	1112	1453	0.282467
121	565	0.05204	0.00125	0.282319	0.000093	–4.7	1349	1844	0.282305
145	563	0.09223	0.00199	0.282459	0.000087	0.6	1151	1522	0.282438
82	550	0.06448	0.00143	0.282486	0.000087	1.0	1112	1467	0.282471
12	543	0.08311	0.00180	0.282346	0.000065	–3.4	1289	1762	0.282328
133	530	0.04132	0.00105	0.282433	0.000098	–1.0	1169	1574	0.282423
38	514	0.04271	0.00096	0.282254	0.000079	–8.2	1437	2022	0.282244
2	507	0.06262	0.00129	0.282297	0.000083	–6.2	1360	1901	0.282285
13	493	0.07442	0.00160	0.282438	0.000087	–2.4	1202	1650	0.282423

Grain numbers correspond to those in Tables 2 and 3. T, $^{206}Pb/^{238}U$ age of zircon. $^{176}Hf/^{177}Hf$, primary isotope ratio recalculated to U–Pb age; $\varepsilon_{Hf}(t)$, deviation of measured $^{176}Hf/^{177}Hf$ ratio from that in CHUR (chondrite reservoir) expressed in ten thousandths. T(DM) and $T(DM)^c$, the model Hf ages of the source calculated taking into account melting of magma from depleted mantle and following the two-stage model based on melting of magma from continental crust.

for melting of A-type granites after suprasubduction–accretionary, collision, syncollision, and postcollision processes (640–520 Ma), which produced S-, I, and A-type granites."

On the other hand, Pystin and Pystina (2011) provide the U–Pb age of 598 ± Ma and interpret it as the age of the Kozhim pluton. Unfortunately, it is unclear whether different authors sampled the same areas of the pluton: the U, Pb, and Th contents of both samples strongly differ and the published data show that the Kozhim pluton can host bodies of different composition and age.

The $\varepsilon_{Hf}(t)$ values of zircons of the Kozhim pluton (complex) strongly vary from –2 to –3.4, indicating a heterogeneous substrate. Some authors ascribe the Kozhim granites to A-type, which makes them similar to granitoids of phase II of the Salner–Mankhambo complex. There are, however, certain differences: the $\varepsilon_{Hf}(t)$ value of rocks of the Salner–Mankhambo Complex is higher (4–10), and a significant part of the Kozhim compositions evidently corresponds to I-type granites (Fig. 3).

The U–Pb age of granites of the Vangyr pluton is 598 ± 5 Ma (Kuznetsov and Udoratina, 2007); these rocks correspond to I-type granites and are close to suprasubduction rocks by petrochemical parameters. They have positive $\varepsilon_{Hf}(t)$ values (2–6) suggesting the presence of mantle material in the substrate. Some compositional features and the presence of older cores in zircons (1224 Ma) indicate a certain role of a sedimentary component in the substrate. In the opinion of O.V. Udoratina, the granites of the Vangyr pluton formed in an active continental margin or an ensialic island arc (Kuznetsov and Udoratina, 2007).

The mostly heterogeneous parameters among these plutons are typical of granites of phase II of the Salner–Mankhambo Complex, which exhibit convergent geochemical characteristics (boundaries of fields, variable substrate). Kholodnov et al. (2022) showed that they formed at the high degree of plume-lithospheric interaction. One of the most important indicators of the latter is related to a low Y/Nb ratio (1.2 and lower) (Fig. 12). According to (Udoratina et al., 2021), the granites of this complex intruded at a postcollision extension stage prior to the opening of the Protouralian Ocean; there is also a viewpoint on the existence of a transform divergent margin at ~520 Ma in the Mankhambo Block (the south of the Lyapin Anticli-

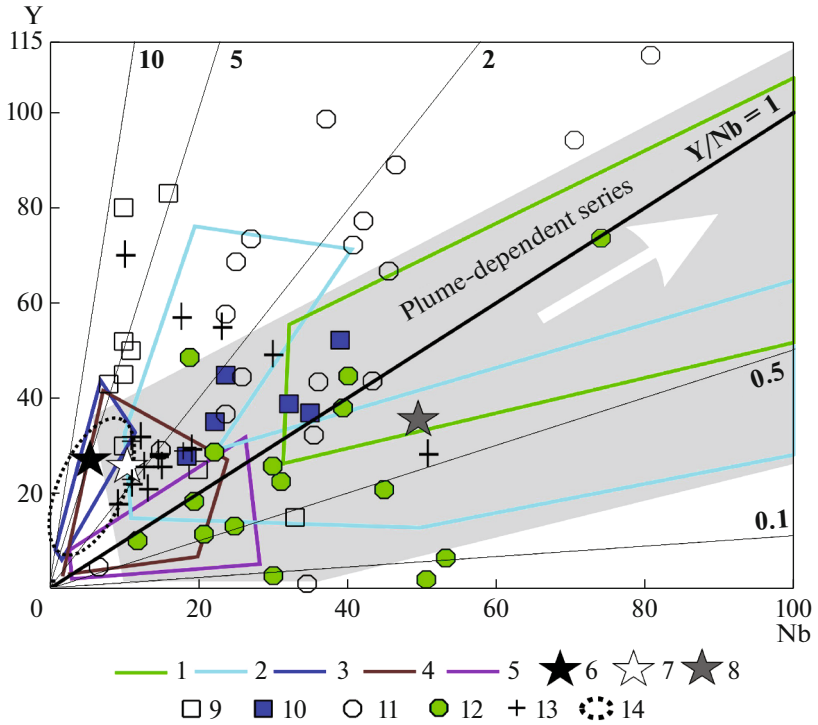

Fig. 12. Summarized Y–Nb diagram for the main geodynamic types of Uralian granitoids. Summarized fields are given after (Kholodnov et al., 2021). (1) Middle to Late Riphean intraplate riftogenic plume-dependent series (western slope of the Urals, margin of the East European Platform); (2) Vendian–Cambrian plume-dependent series of the "Timan" stage: Isherim, Lyapin, and other anticlinoriums; (3) Late Ordovician–Middle Devonian island-arc series; (4) Late Devonian–Late Carboniferous suprasubduction marginal-continental gabbro–tonalite–granodiorite–granite series, Central Urals (Upper Iset, Shartash, Kamenushka plutons, etc.); (5) Early–Middle collision crustal–anatectic granitic series (Dzhabyk, Murzinska, Adui plutons, etc.); (6) N-MORB; (7) E-MORB; (8) OIB after (Sun and McDonough, 1989); (9, 10) granitoids from the (9) Vangyr and (10) Kozhim plutons; (11, 12) phases I and II of the Salner–Mankhambo Complex; (13) Vodorazdelny pluton; (14) rhyolites of the Mount Sablya Complex (Kuznetsov and Udoratina, 2007; Dushin et al., 2017; Udoratina et al., 2020). Gray field combines the main plume-dependent Urals granitoid series of various ages (Kholodnov et al., 2021).

norium), which is consistent with the first viewpoint by the movement types. This stage was probably started from felsic (sub)volcanic rocks in the structure of the Mount Sablya Formation, the geochemical parameters of which partly correspond to A-type granites. Their formation could have been related to the first plume influence (the Y/Nb ratio of ~1; position close to OIB) with the remaining contribution of subduction and crustal contamination (Kholodnov et al., 2022).

What is the position of granites of the Vodorazdelny pluton in this range of rocks? For comparison, we plotted the compositions of rocks of the Vodorazdelny, Kozhim, and Vangyr plutons and two phases of the Salner–Mankhambo Complex, as well as subvolcanic rhyolites (which determined the age of the Mount Sablya Formation of 494–583 Ma; Kuznetsov and Udoratina, 2007; Dushin et al., 2017; Udoratina et al., 2020), which are discussed below.

Among three age clusters recognized for granites of the Vodorazdelny pluton (502 ± 7, 548 ± 5, and 593 ± 5 Ma), in our opinion, the age of the rock is 593 ± 5 Ma on the basis of the peculiarities of the chemical composition, the degree of preservation, and the inner structure of zircon grains. It almost coincides with the age of granites of the Vangyr pluton, which is located within the same segment of the Lyapin Anticlinorium (Ivanov et al., 2013a) and ascribed to the Salner–Mankhambo Complex.

In SiO_2 contents, the granites of the Vodorazdelny pluton are most similar to rocks of phase I of this complex. In the Vangyr and Kozhim plutons, the rocks with higher SiO_2 content are dominant; however, this can also indicate a different degree of erosion or an insufficient set of analyses. Within a range of SiO_2 contents of 70–77 wt %, the granites of these (including the Vodorazdelny) plutons and rocks of phase I of the Salner–Mankhambo Complex have similar Rb, Sr, Hf, Ta, and Th contents. The granites of the Vangyr and Vodorazdelny plutons are the most similar according to the content of key elements (Y and Nb) and their ratio: the Y/Nb ratio of most samples is 2–5, which is close to the position of an E-MORB source and is typical of suprasubduction rocks, as was shown by Kholodnov et al. (2022). Note that the Vodorazdelny pluton contain samples with higher Y and Nb

contents and the Y/Nb ratio of one sample of <1. All these facts can indicate a heterogeneous substrate or contamination events.

The rocks of phase II of the Salner–Mankhambo Complex significantly differ from the aforementioned granites with respect to the contents of all key elements and their Y/Nb ratio is close to that of OIBs corresponding to plume-dependent rocks. By the Y/Nb ratio, the rocks of the Kozhim pluton occupy an intermediate position (the Y/Nb ratio of 1–2), which can indicate a mixed source type (OIB + E-MORB). According to Puchkov (2000) and Kholodnov et al. (2022), an increasing role of the OIB component in the source can indicate the influence of a plume factor (material + energy?) in generation of granitoids.

It is considered (Faure, 1989; Martynov, 2010) that suprasubduction magmas could mainly be sourced from rocks of a mantle wedge, a "subduction component" (fluids) that originated upon dehydration of slab material, and melts that formed upon melting of basic rocks and sediments of the subducted oceanic plate. The composition of the mantle component, which is not modified by subducted fluid, can be characterized by ratios of some elements inert in the fluid phase: Nb/Yb, Ta/Yb, etc. The Y/Nb values of rocks of the Vodorazdelny pluton are 4–8, which is significantly higher than in MORBs (Nb/Yb = 0.76; McDonough and Sun, 1995), indicating possible melting of initially richer mantle substrate rather than depleted mantle. The high Th/Yb values (3–9) indirectly point to the contribution of a subduction component to the formation of granites of the Vodorazdelny pluton. Because granites are crustal rocks, their pattern of trace elements can be affected by other factors. For example, the enrichment of granites in Th (relative to the oceanic basalts) can be triggered by the presence of sedimentary sequences or older granitoids (gneisses) in the crustal melting source. The indirect impact of mantle processes on the composition of crustal granites can occur through partial melting of mantle mafic rocks or mixing of mantle magmas and fluids with crustal material in secondary melting sources. By the $(La/Yb)_n$–Yb ratio (Martin, 1993), most compositions of granites of the Vodorazdelny pluton correspond to "classical island-arc rocks," which can also indirectly indicate the mafic component of the substrate.

Figure 13 also shows some other correlations allowing us to refine the role of subduction and plume factors. In addition to the compositions of granites from the Subpolar Urals, this figure shows the fields of typical suprasubduction Paleozoic granites of the Uralian Orogen, as well as the plume-dependent granitoids from its various sectors (our database). Here we can also see similar compositions of granites of the Vodorazdelny and Vangyr plutons and their similarity to suprasubduction rocks, whereas the granites of both phases of the Salner–Mankhambo Complex lie in the fields of plume-dependent rocks and the Kozhim granites occupy an intermediate position. The Ba content of granites of the Vodorazdelny pluton is relatively low, which is related either to the postmagmatic alterations or Ba removal upon alteration of oceanic basalts involved as a substrate component (Yan et al., 2019). Because of this, the granites of the Vodorazdelny pluton have a lower Ba/La ratio (8, on average), the high value of which is an important characteristic of suprasubduction rocks (>30; Fershtater, 2013). Note that heterogeneity and similarity of some compositions to plume-dependent granites can be traced on all diagrams for the compositions of granites of the Vodorazdelny pluton. On the other hand, they are close to the composition of the upper continental crust (Fig. 5b) and collision rocks (Fig. 4) in the ratios of some elements, which indicates a important amount of sialic material in their genesis.

In our opinion, the complex of geochronological, petrogeochemical, and isotopic data do not allow us to ascribe the granitoids of the Vodorazdelny and Vangyr plutons to phase II of the Salner–Mankhambo Complex. The granites of the Vodorazdleny pluton are similar by some parameters to rocks of phase I of this complex and significantly differ from it according to other features. The age of these plutons is older, the substrate is heterogeneous, the petrochemistry is clearly "suprasubduction," and the compositions show no impact of a plume factor (see the ratios of components in Figs. 12 and 13). It is likely that these are still not collision or postcollision rocks; they were generated at the final stages of evolution of a continental margin (possibly, upon transition from subduction to intraplate setting; Aplonov, 2001) and represent an individual episode of granite formation at the Subpolar Urals.

It is correct to relate the granites of the Kozhim pluton, at least those of them whose compositions are closer to those of granites of the Vangyr and Vodorazdelny plutons rather than to those of rocks of phase II of the Salner–Mankhambo Complex on many petrochemical diagrams, to the first two rocks. Assuming the age of 598 Ma, we thus support Pystin and Pystina (2011) that a granitoid complex with this age, which should be ascribed to the end of the Neoproterozoic (Ediacaran, 635–541 Ma; Cohen et al., 2013) or the Vendian according to Uralian subdivisions (Semikhatov et al., 2015), should be recognized upon geological mapping. Whether this complex should be named "Kozhim" is debatable, because the granitoid bodies within the Kozhim pluton could be heterogeneous.

In opinion of some authors, the question of relation of granites of the Vodorazdelny pluton to rocks of the Mount Sablya Formation, as well as the composition, occurrence halo, and the age of the latter, remains open. An intrusive contact of the Vodorazdelny pluton (west) with rocks of this formation is shown on the map according to a survey of 1982 (Dashkevich and Gesse, 1982). In the latest edition of

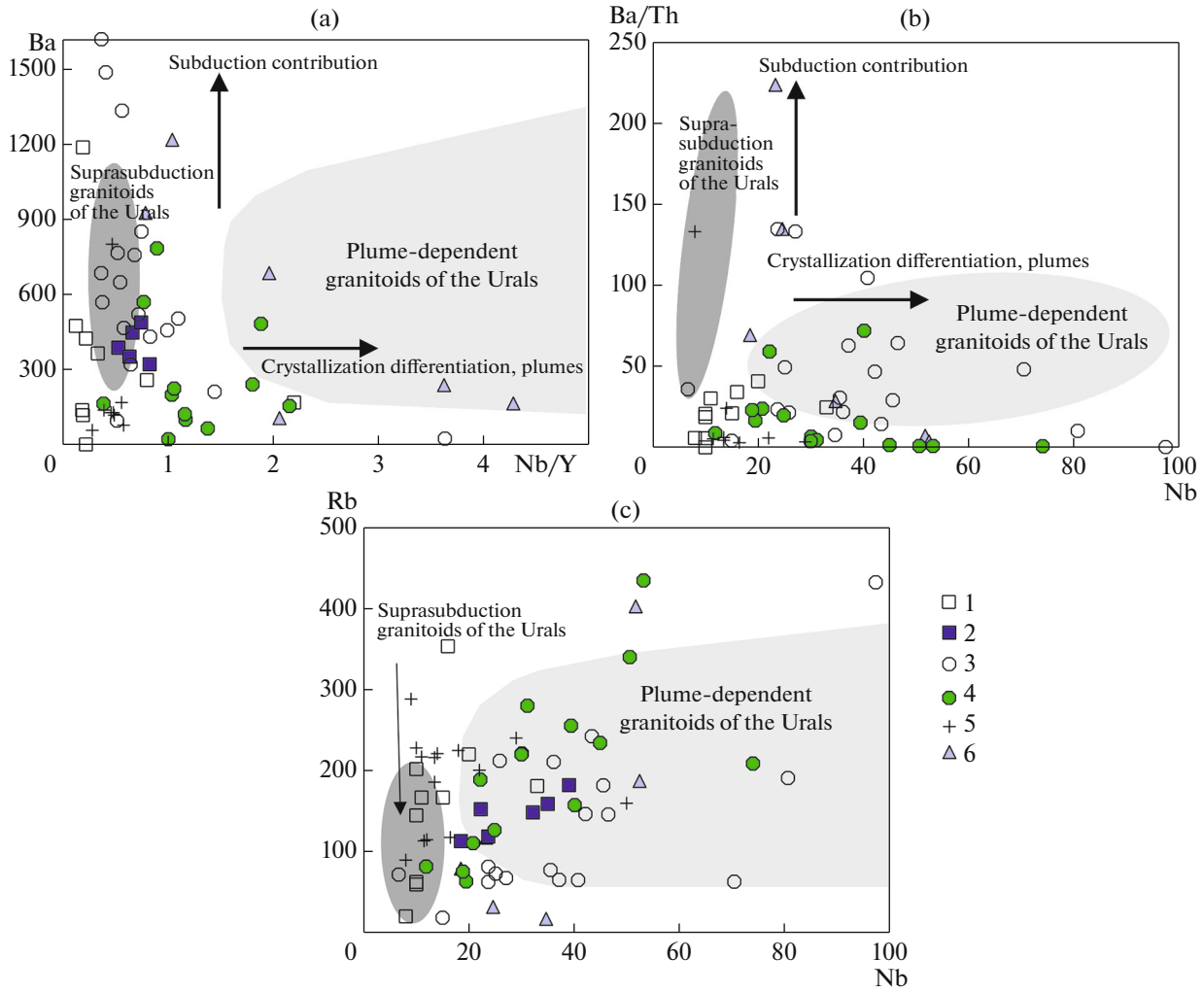

Fig. 13. Correlations of trace elements characterizing the contribution of various sources and processes to petrogenesis of felsic rocks of the Vodorazdelny pluton and its possible analogs. Diagram in Fig. 13a is taken from (Kepezhinskas et al., 1997); diagrams in Figs. 13b and 13c are original combinations of indicator elements also reflecting the contribution of various sources to petrogenesis of granites (Kholodnov et al., 2022). Using our database, we plotted the compositions of granitoids of the Uralian Orogen: typical representatives of suprasubduction (Upper Iset, Shabry, Sukhovyaz, Krasninskii, and many other plutons, 148 samples, dark gray field) and plume-dependent formations (Stepnoi, Uvildy, Kozlinaya Gora (Kozlinogorskii), and other plutons, 50 samples, light gray field). For legend, see Fig. 2.

the State Geological Map (Ivanov et al., 2013a), the western contact of the pluton is cut by a fault and the Mount Sablya Formation is not shown at the contact with the Vodorazdelny pluton (although the text mentions this contact); the granites of this pluton in the north have contact with the Ar'yanshor Sequence containing Vendian microfossils. "In the southwestern angle of the area of the sheet (Q-40-XXX, author's remark), the rocks of the Ar'yanshor Sequence conformably overlap the felsic volcanic rocks of the Mount Sablya Formation; in other cases, 'the variegated rocks' occur with erosion on shales of the Moroya or quartzites of the Khobeya formations..." (Ivanov et al., 2013a). It is mentioned that the contacts of the Vodorazdelny pluton with country rocks are "sinuous, uneven, sharp." The ages of rocks of the Mount Sablya Formation are as follows. The zircons from metarhyolites and metabasalts of a volcanic halo of the Mount Sablya Formation and the upper reaches of the Pechora River exhibit two age groups: 583 ± 4 and 495 ± 5 Ma. The lower and upper intercepts of discordia with concordia yielded 478 ± 150 and 591 ± 150 Ma (SHRIMP-2), respectively (Il'yasova et al., 2017). The authors of this paper thus consider that rhyolites are Vendian, whereas the younger zircon grains formed later owing to a tectono-thermal event. The compositions of metabasalts do not correspond to the agreement line indicating disturbed isotope ratios. "The discordia line yielded the age of 547 ± 27 Ma (n = 12, MSWD = 0.75), which can correspond to the age of crystallization of basalts" (Il'yasova et al., 2017). There are the earlier ages of zircons from the rocks ascribed to the Mount Sablya Formation: 642 Ma from felsic effusive rocks of the Maly Patok region

(Chervyakovskiy et al., 1992) and 586 ± 12 Ma from volcanic rocks of the Maldy-Nyrd Range (Volchek, 2004); the TIMS age of zircons from rhyolites of this range is 519 ± 17 Ma (Soboleva, 2004). The LA-ICP-MS age of metarhyolites of Mt. Neilentump is 586.3 ± 4.3 Ma (Il'yasova et al., 2017).

A wide age range allows the authors of the map of sheet Q-40-XXX to suggest that the Mount Sablya Formation contains Vendian and Late Cambrian volcanic rocks or that all values of ~494 Ma reflect the age of metamorphism. In their opinion, the question on the age of metavolcanic rocks ascribed to the Mount Sablya Formation requires further study.

The ages of ~494 Ma occur in zones of zircons from various objects: metabasalts of a southern halo of the Mount Sablya Formation and granitoids of the Salner–Mankhambo Complex (Dushin et al., 2017). Similar (within the error) age clusters are detected in zircons of the Kozhim and Vodorazdelny plutons. We thus agree with a conclusion on the stage of metamorphism of rocks of the Mount Sablya Formation (and our studied plutons) in the indicated range. Let us recall that the altered zircons of the Vodorazdelny pluton also contain the population of 548 ± 5 Ma, the age of which is almost identical to a "hypothetical" age of crystallization of basalts of the Mount Sablya Formation (see above). It is thus likely that this also reflects the age of a metamorphic event superimposed on older rocks.

The petrochemical peculiarities of subvolcanic rocks of the Mount Sablya Formation, nonetheless, allow us to compare them (by source and geodynamic regime) with granites of the Vodorazdelny and Vangyr plutons, as well as to accept that the Mount Sablya volcanic rocks are intruded by these granites. In our opinion, the rocks of the Mount Sablya Formation are poorly studied and could combine the rocks of various ages and even genesis. This is evident from their heterogeneous composition (Kholodnov et al., 2022) similar to that of granites combined into phases I and II of the Salner–Mankhambo Complex, in which the plume and crustal components probably interacted synchronously at various levels and proportions. Similar parameters (in particular, the Y/Nb ratio) indicate the presence of the OIB component in the protolith of the Mount Sablya rhyolites, which is typical of plume-dependent igneous rocks, e.g., granites of the Salner–Mankhambo Complex. The latter is significantly younger (~520 Ma) than the granites of the Vodorazdelny and Vangyr plutons, which are characterized by "suprasubduction" geochemical parameters, as was shown above. The last two conclusions are consistent, because the Timan orogenesis in this sector followed subduction. The real ages of the Mount Sablya Formation, in our opinion, could therefore be younger than the age of granites of the Vodorazdelny pluton (598 Ma) and lie within a range of 583–568 Ma (Early Vendian), whereas the composition of rocks combined into this formation requires more detailed consideration. The U–Pb age of zircons from subvolcanic trachyrhyolites of the overlying (unconformably?) Laptopai Formation is 554 ± 4 and 556 ± 11 Ma (Dushin et al., 2017).

If we accept the viewpoint of Kuznetsov (2009) and Kuznetsov et al. (2017) that the beginning of the Cambrian was characterized by collision of the Baltic (part of the basement of the present-day East European Platform) and Arctida continents, then the suprasubduction granitoids of the conditional "Kozhim complex" (Vodorazdelny, Vangyr, and Kozhim plutons, in particular) referred to as proto-Uralides "are the compositional results of subduction beneath the Bolshaya Zemlya active margin of Arctida, whereas ... the I-type rocks with the age of 560–515 Ma mark the stage of collision of the Timan passive margin of Baltic and the Bolshaya Zemlya active margin of Arctida" (Kuznetsov et al., 2007). Further intrusion of A- and S-type granitoids (including Mount Sablya rhyolites) was related to collision and postcollision divergent processes and probably plume activity. Our data are in agreement with this viewpoint, excluding (in case of the Vodorazdelny pluton) the influence of the plume factor.

Composition of Substrate for Melting of Granitoids of the Kozhim Block

Let us consider indirect data allowing some assumptions on the substrate for melting of granites of this block. The compositions of rocks of the Vodorazdelny (as well as Vangyr) pluton form a field shifted from the area of metapelites to the field of metagreywackes (Fig. 14c); some compositions lie close to an influence zone of a metamafic substrate. By Rb, Ba, and Sr relationship (Fig. 14d), the compositions of the studied rocks occur in a basaltoid field. The index correlations of zircons (Figs. 14a, 14b) also indicate the significantly oceanic type of substrate for granites of the Vodorazdelny pluton. Poor data on the content of trace elements in selected grains of zircon of the Kozhim pluton show that their compositions lie in the field of continental zircons. As was shown above, however, this pluton (or part of its granites) can be younger and could have been generated upon change of the geodynamic regime and thus from another source.

The interpretation of the substrate for many granitoids of the Subpolar Urals, in particular, for those abundant within the Lyapin Anticlinorium (Udoratina et al., 2021; Kholodnov et al., 2022) is ambiguous. Kholodnov et al. (2021, 2022) applied the Y–Nb diagram to identify the differences between granites of various geodynamic settings and to preliminarily estimate the composition of the substrate, including for felsic rocks. The heterogeneous substrate of the Vodorazdelny pluton is emphasized by a series of facts. On one hand, most compositions of granites of the pluton correspond to oceanic rocks on diagrams which link the chemical composition of zircons with the composition

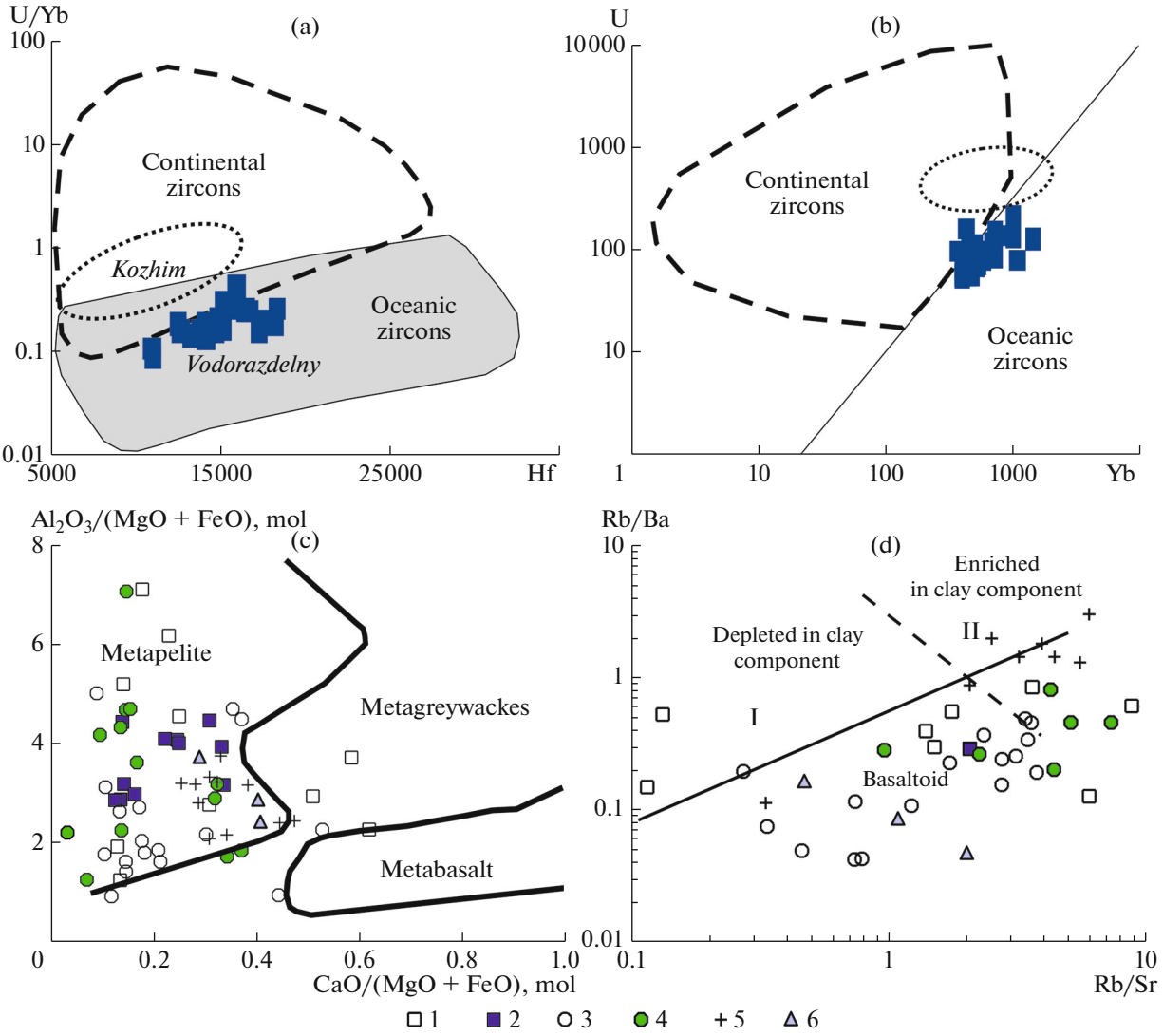

Fig. 14. Diagrams for determination of the composition of the substrate for melting of granitoids. (a, b) By rock composition (Sylvester, 1998; Altherr et al., 2000); (c, d) by composition of zircons (Grines et al., 2007). For legend, see Fig. 2.

of substrate, indicating the influence of a mafic constituent in the substrate. The low Y/Nb value of granites of the studied pluton is close to that of E-MORBs, but the levels of contents of these elements vary strongly. The Na_2O/K_2O ratio is >0.5, which indicates a magmatic character of the protolith according to Chapell and White (1992). On the other hand, the zircons of the Vodorazdelny pluton contain many ancient cores with the U–Pb age of 2190–780 Ma, which means the involvement of the continental basement material in their formation. It is important to note that detrital igneous zircons with these ages (2060–900 Ma) are abundant in the Upper Riphean and Lower Paleozoic sandstones of the Polar Urals and South and Central Urals, which formed owing to long erosion of the northeastern margin of the East European Craton (Kuznetsov et al., 2010; Andreichev et al., 2013; Krasotkina et al., 2020). The granites of the Vodorazdelny pluton are peraluminous, which also indirectly indicates the presence of metasedimentary material in the substrate.

The Lu–Hf isotopic data of zircons should serve as the most reliable indicators of the composition of the substrate, because this system is unaffected by superimposed processes. The behavior of Lu and Hf isotopes in zircons of granites of the Vodorazdelny pluton allows the following conclusions. The cores with high positive $\varepsilon_{Hf}(t)$ values and the Paleo- and Mesoproterozoic age of 2189 and 1599 Ma indicate the involvement of juvenile material (Table 4). The compositions of these zircons are located significantly above the DM line, which is relatively rare, and the high $\varepsilon_{Hf}(t)$ values for rocks of this age can be an analytical artifact. A list of possible analytical errors of this method using a similar class of equipment is described by (Lokhov et al., 2009) and was taken into account in our case;

thus, they should not occur. We provide these results in Table 4 and are planning to conduct an additional study of zircons of similar exterior and morphological type and to confirm or reject these data.

An exotic explanation of extreme Hf behavior is given by Lokhov et al. (2009) for calciphires of the Okhotsk pluton ($\varepsilon_{Hf}(t) = 87$). It is suggested that the protomaterial of the Earth (Enrich Hadean Impact Differentiates) underwent thermal differentiation and influence of fluids with a high Lu–Hf ratio and was further assimilated by most ancient volcanic rocks, was partly buried by them, became part of the lithospheric mantle, and was not involved in deep convection and, therefore, could not have been preserved (Lokhov et al., 2009).

The $\varepsilon_{Hf}(t)$ value of the Mesoproterozoic zircon (1354 Ma) from granites of the Vodorazdelny pluton is very low (0.8), indicating a more crustal source close to CHUR for this grain. These could have been the rocks of the basement of the continental block, which was further involved in the structure of the East European Platform. This value coincides with the age of the Mashak riftogenic event, which was accompanied by the formation of a significant amount of igneous rocks of various depths (basalts and rhyolites of the Mashak, Kuvashi, and Shatak formations, gabbroids and granites of the Kusa-Kopan intrusion, etc.) at ~1389–1350 Ma in the South Urals (in the present-day coordinates). Xenogenic cores with such dates were established in Paleozoic granites of the Bashkirian Meganticlinorium (Shardakova, 2016).

The Neoproterozoic zircon rims (632 and 612 Ma), in our opinion, are the alteration products and were probably formed from fluid (or evolved melt) with "mantle" characteristics; thus, their $\varepsilon_{Hf}(t)$ values are weakly positive (around +2). It is known that the Hf isotopic composition of metamorphic zircons either is inherited from igneous zircons or can be more radiogenic owing to the exchange with coexisting mineral phases or the melt (Gerdes and Zeh, 2009; Chen et al., 2010). There is a cluster of zircons with ages of 619 ± 9.1 Ma within the Kozhim pluton (485 Ma), which is considered "inherited from the previous stage" (Udoratina et al., 2020).

The variations in Hf isotopic composition between the individual grains of igneous zircon marking the age of granites of the Vodorazdelny pluton reflect the contribution of crustal material to magma formation. All of them, excluding grain 77 (see above), are characterized by $\varepsilon_{Hf}(t)$ values around zero (–2 to 0 to +1) close to the CHUR line.

Judging from isotopic characteristics, the zircon grains (zones) with younger age than that corresponding to the age of the rock (Table 3) underwent various tectono-thermal impacts. Some of the grains (565–530 Ma) inherit the characteristics of igneous zircons weakly varying by the degree of crustal affinity; the younger grains (514–593 Ma) accumulated radiogenic Hf, providing higher negative $\varepsilon_{Hf}(t)$ values (–6, –8). These two zircon types were probably generated upon individual episodes of tectono-thermal activity, in our opinion, coinciding with activity pulses of a mantle plume ("Mankhambo plume"; Puchkov, 2018), which ascended from the lower horizons and could have served as the energy source initiating crustal melting and/or separation of the fluid phase, which affects the Lu–Hf isotopy of zircons. The link between the formation of granites of the Lyapin Anticlinorium and the ages of 540–480 Ma is substantiated in a number of works (Puchkov, 2018; Kholodnov et al., 2022). In any case, nobody questions the presence of several pulses of granite formation in this structure, which occurred after 598 Ma not in an active convergent margin setting.

The substrate involved in the generation of granites of the Vodorazdelny pluton was thus mixed with a material of variously depleted mantle and ancient crust. The two-stage model ages of igneous zircons vary in a range of 1699–1251 Ma (Fig. 12b); the same range also contains part of the ages of ancient grains with different $\varepsilon_{Hf}(t)$ values (see above). The model ages for the most ancient zircons with "mafic" substrate even calculated following a one-stage model ($T_{Hf}(DM)$ for points 130 and 97) could not correctly be estimated. Our values are much lower than the age of zircons, which indicates a disturbed isotopic system (?). At the same time, the model age for zircons of the Vodorazdelny pluton, which has the age of the "Mashak" event (1354 Ma, point 16, Table 3) and the $\varepsilon_{Hf}(t)$ value of 0.8, yields the "real" ancient $T_{Hf}(DM^c)$ value of 2080 Ma, supporting that the material with this age occurred during the process of recycling.

The analysis of petrogeochemical, geochronological, and isotopic data on igneous rocks of the entire Lyapin Anticlinorium shows that the isotopic characteristics of rocks of the complexes formed in the period of 650–480 Ma are strongly variable (Udoratina et al., 2021). This can be traced by example of the Vangyr, Kozhim, and Mankhambo plutons (in the structure of the Salner–Mankhambo Complex) used for the comparison with the Vodorazdelny pluton. In spite of variously interpreted ages of crystallization of rocks, almost all granites (as well as in the Vodorazdelny pluton) have Late Riphean–Vendian zircons. In all objects (except for the Vodorazdelny pluton), the relatively young values (485, 598, and 522 Ma for the Kozhim, Vangyr, and Mankhambo plutons, respectively) are considered the age of the rocks, whereas the older ages are inherited from the previous stage (i.e., the zircons of the substrate were preserved or were trapped from country rocks). The ancient zircons (1224 Ma) are registered in the Vangyr pluton and the Hf model ages $T_{Hf}(DM^c)$ for its granites are 1.76–1.32 Ma. We should also remember the U–Pb age of zircon of 1390 Ma (Dushin et al., 2012), which was accepted as the age of rocks of phase I of the pluton, because the Nd model age of granites (1.42 Ga) almost

coincided with it. According to new data (Udoratina et al., 2021), the $T_{Hf}(DM^c)$ values of rocks of the Kozhim pluton and phase II of the Mankhambo pluton are 1.41–1.07 Ga and are 2.05–1.31 Ga for leucogranites of phase II of the Mankhambo pluton. In addition to a currently approved age of 522 Ma, the Cambrian (510, 501, and 489 Ma) and even Paleozoic (253.3 Ma) concordant values for zircon clusters are also provided for granites of the Mankhambo pluton (Dushin et al., 2017). All this is probably influenced by later tectono-thermal activity.

It is important to recall that clear "suprasubduction" geochemical parameters among the Vangyr, Kozhim, and Mankhambo plutons are typical only of the Vangyr pluton; the other two younger plutons were ascribed to the next stage of evolution of the Timanides (Udoratina et al., 2021). Nonetheless, the positive $\varepsilon_{Hf}(t)$ values of zircons from all these granitoids, as well as in the Vodorazdelny pluton, indicate the presence of a mafic component in the substrate for melting of granitoids. Its nature can be diverse. In the case with the Vangyr and Vodorazdelny plutons, there is partly ancient juvenile mafic material (if we take into account the high $\varepsilon_{Hf}(t)$ values for ancient zircons) + the involvement of mafic rocks (and sediments) of slab and fluid separated upon dehydration of slab rocks + the crustal component. For the Kozhim pluton and phase I of the Mankhambo pluton, we can suggest an indirect involvement of the material of a previously detached slab which was deeply submerged into the mantle. It could have melted, producing the basaltic, picritic, or andesitic magmas, the uplift of which to the crustal area was responsible for the formation of granite-producing magmatic sources. Additional sources could have included material (and energy) of mantle plume and fluid separated from slab.

On the basis of our new data, which supplement the available isotopic-geochemical information on granites of the Subpolar Urals, it can be concluded that the granitoids of similar age but of different geodynamic evolution stages of this sector inherit the composition of the substrate in spite of similar and distinct geochemical features. This results in a variable amount of mafic component in the source. This again contradicts a recent viewpoint on a pure crustal anatectic nature. For example, the study of Sr isotopic composition of Cambrian granites of the Subpolar Urals (Dovzhikova, 2007) showed very high values of primary $(^{87}Sr/^{88}Sr)_i$ ratios of 0.71–0.75. It was also considered that the significant volumes of A-granites could not have melted without more mafic rocks down the section. Many petrogenetic models suggest the origin of A-granites only from sialic material, but there is no experimental proof of melting products close in composition to A-granites from the crustal material (Bonin, 2007).

The episodes of granitic magmatism of the Lyapin Anticlinorium repeated in a range of the Middle Riphean–Vendian–Early Cambrian during the origination of the Subpolar Uralian segment of the crust. They were accompanied by the processes of multistage high-temperature metamorphism (Pystin and Pystina, 2008), which were also present during later Timan orogenic events, and resulted, in addition to common geological features, in the formation of several generations of zircons (or their zones) in granitoids of this age. The ages of relict zircons (2100, 1599, and 1354 Ma for the Vodorazdelny pluton) indicate the role of ancient material in their substrate.

New data on various isotopic systems for granites of various parts of the current structure of the Uralian mobile belt and its northeastern frame (Udoratina et al., 2021; Kholodnov et al., 2022) indicate the lesser amount of granites with pure sialic substrate, as was considered before.

CONCLUSIONS

(1) By petrogeochemical characteristics, the granites of the Vodorazdelny pluton (as well as the nearby Vangyr pluton) are similar to suprasubduction rocks. The ratios of key elements show the presence of mafic material of a melting slab, as well as high-Al sialic material, in the composition of the substrate of melting source.

(2) On the basis of the U–Pb age of the main population of zircons from granites, we substantiated the Vendian (Ediacaran) age of the Vodorazdelny pluton of 593 ± 4.3 Ma. This age within the error coincides with the age of granites of the nearby Vangyr pluton (598 ± 5 Ma), as well as the ages of cores of zircons that are present in a series of Cambrian plutons of the Lyapin Anticlinorium (Kozhim and Keftalyk, etc.).

(3) The ancient Paleo- and Neoproterozoic cores are found in zircons of the Vodorazdelny pluton. One of them (1599 Ma) has high $\varepsilon_{Hf}(t)$ values, which can indicate the involvement of melted or trapped grains from ancient mafic material (?); in other, younger, grains (1354 Ma), the important role is played by the crustal ($\varepsilon_{Hf}(t) = 0.8$) component (the material of the basement of ancient platform).

(4) The $\varepsilon_{Hf}(t)$ values of zircons, the ages of which are accepted by us as the age of granites of the Vodorazdleny pluton, vary around zero, indicating the heterogeneous source (mantle and crustal material) of melts. The $\varepsilon_{Hf}(t)$ values of granites of the Vangyr pluton similar in composition are significantly higher (2–6). The marginal zones of zircons from granites of the Vodorazdleny pluton formed during later tectonothermal processes, the age of which coincides with episodes of Early Cambrian granite formation in the Lyapin Anticlinorium, partly inherit the isotopic parameters of granites, and further, as they become younger, their signatures are shifted toward the more crustal source ($\varepsilon_{Hf}(t) > -8$).

(5) The age and petrogeochemical peculiarities of granites (as well as their zircons) do not support the

referral of the Vodorazdelny pluton, as well as its analogs (Vangyr pluton and some rocks of the Kozhim pluton), to the Salner–Mankhambo Complex and again indicate the possibility of the presence of a subdivision with the age of ~598 Ma as was suggested by Pystin and Pystina (2011).

(6) The composition and the age of rocks combined into the Mount Sablya Formation require further detailed studies.

(7) The presence of several stages of granite formation (Middle Riphean–Vendian–Cambrian) and accompanying metamorphism and the complex structure of metamorphic rocks in the basement of the Lyapin Anticlinorium lead to variable isotopic parameters characterizing the heterogeneous melt source, on one hand, and convergent geochemical features, on the other hand.

ACKNOWLEDGMENTS

The first routes in the Vodorazdelny pluton were conducted together with a field team of S.G. Chervyakovskiy, who was a famous geologist and an expert of the Subpolar Urals.

FUNDING

This work was supported by state contracts of the IGG UB RAS nos. 123011800009-9 and AAAA-A19-119072990020-6. Reequipment and complex development of the Center for Collective Use Geoanalitik of the IGG UB RAS is supported by the Ministry of Science and Higher Education of the Russian Federation, project no. 075-15-2021-680.

CONFLICT OF INTEREST

The authors declare that they have no conflicts of interest.

Reviewers A.B. Kuznetsov and G.A. Petrov

REFERENCES

Altherr, R., Holl, A., Hegner, E., Langer, C., and Kreuzer, H., High-potassium, calc-alkaline I-type plutonism in the European Variscides: Northern Vosges (France) and northern Schwarzwald (Germany), *Lithos*, 2000, vol. 50, pp. 51–73.

Andreichev, V.L., Gechronology of granitoid magmatism of the Subpolar Urals, *Vestn. IG Komi NTs UrO RAN*, 2010, no. 11, pp. 7–12.

Andreichev, V.L., Soboleva, A.A., and Gehrels, G.E., U–Pb age of detrital zircons from the Upper Precambrian terrigenous section of North Timan, *Dokl. Earth Sci.*, 2013, vol. 450, no. 2, pp. 592–596.

Aplonov, S.V., *Geodinamika* (Geodynamics), St. Petersburg: SPbGU, 2001 [in Russian].

Balashov, Yu.A. and Skublov, S.G., Contrasting geochemistry of magmatic and secondary zircons, *Geochem. Int.*, 2011, vol. 49, no. 6, pp. 594–604.

Belousova, E.A., Griffin, W.L., O'Reilly, S., and Fisher, N.I., Igneous zircon: Trace element composition as an indicator of source rock type, *Contrib. Mineral. Petrol.*, 2002, vol. 143, pp. 602–622.

Bonin, B., A-type granites and related rocks: Evolution of a concept, problems and prospects, *Lithos*, 2007, vol. 97, pp. 1–29.

Chappell, B.W. and White, A.J.R., I- and S-type granites in the Lachlan Fold B, *Trans. R. Soc. Edinburg Earth Sci.*, 1992, vol. 83, pp. 1–26.

Chen, R.-X., Zheng, Y.-F., and Zie, L., Metamorphic growth and recrystallization of zircon: distinction by simultaneous in-sity analyses of trace elements, U–Th–Pb and Lu–Hf isotopes in zircon from eclogite-facies rocks in the Sulu orogen, *Lithos*, 2010, vol. 114, pp. 132–154.

Chervyakovskaya, M.V., Votyakov, S.L., and Chervyakovskiy, V.S., Study of Lu/Hf isotopic composition of zircons using a Neptune Plus multicollector inductively coupled plasma mass spectrometer with an NWR 213 laser ablation attachment, *Analitika Kontrol'*, 2021, vol. 25, no. 3, pp. 212–221.

Chervyakovskaya, M.V., Chervyakovskiy, V.S., and Votyakov, S.L., LA-ICP-MS analysis of trace elements in silicate minerals on ON ICP-MS NEXION 300S mass-spectrometer with NWR 213 attachment for laser ablation: Methodological aspects, *Geodynam. Tectonophys.*, 2022, vol. 13, no. 2s, pp. 1–8.

Chervyakovskiy, S.G., Ivanov, V.N., Kurzanov, I.Yu., Kuzenkov, N.A., and Ronkin, Yu.L., On the age of the Malyi Patok granitoid massif (Subpolar Urals) and its formational belonging, in *Ezhegodnik-91. Inform. sb. nauchn. tr. IGG UrO RAN* (Yearbook-1991. Coll. Sci. Works Inst. Geol. Geochem. Ural. Branch Russ. Acad. Sci.), Ekaterinburg: Inst. Geol. Geokhim. Ural. Otd. Ross. Akad. Nauk, 1992, pp. 71–74.

Cohen, K.M., Finney, S.C., Gibbard, P.L., and Fa, J.-X., T The ICS International Chronostratigraphic Chart, *Episodes*, 2013, vol. 36, pp. 199–204.

Dashkevich, G.I. and Gesse, V.N., *Gosudarstvennaya geologicheskaya karta SSSR. Masshtab 1 : 200000. Seriya Severo-Ural'skaya. List Q-40-XXX (Manaraga)* (The 1 : 200000 State Geological Map of the USSR. Ser. North Urals. Sheet Q-40-XXX (Manaraga)), Leningrad: Vseross. Nauchno-Issled. Geol. Inst., 1982 [in Russian].

Dovzhikova, E.G., Late Cambrian magmatism of the Pechora Fault Zone (the central part of the Pechora Plate), *Cand. (Geol.-Mineral.) Dissertation*, Syktyvkar, 2007.

Dushin, V.A., Ronkin, Yu.L., and Lepikhina, O.P., Age and geodynamic position of granitoids of the Man'khambo block (North Urals): U–Pb and Sm–Nd isotope systematics and geochemical constraints, in *Izotopnye sistemy i vremya geologicheskikh protsessov. Mater. IV Ross. Konf. po izotopnoi geokhronologii* (Proc. IV Russ. Isotope Geochronol. Conf. "Isotope Isotope Systems and the Time of Geological Processes"), St. Petersburg, 2009, vol. 1, pp. 125–127.

Dushin, V.A., Koz'min, V.S., Serdyukova, O.P., Nikulina, I.A., and Kolganov, E.R., Geology and rare-metal-uranium-thorium compound mineralization of Mankhambo block (Subpolar Urals), *Litosfera*, 2012, no. 2, pp. 166–172.

Dushin, V.A., Serdyukova, O.P., Malyugin, A.A., et al., *Gosudarstvennaya geologicheskaya karta Rossiiskoi Federatsii. Masshtab 1 : 200000. Izdanie vtoroe. Seriya Severo-Ural'skaya. List P-40-XII (g. Kozhim-Iz). Ob''yasnitel'naya zapiska* (The 1 : 200000 State Geological Map of the Russian Federation, 2nd ed. Ser. North Urals. Sheet P-40-XII (Kozhim-Iz). Explanatory Note), Moscow: Mosk. Fil. Vseross. Nauchno-Issled. Geol. Inst., 2017 (in Russian).

Faure, G., *Principles of Isotope Geology*, 2nd ed., New York: John Wiley, 1986.

Ferry, J.M. and Watson, E.B., New thermodynamic models and revised calibrations for the Ti-in-zircon and Zr-in-rutile thermometers, *Contrib. Mineral. Petrol.*, 2007, vol. 154, pp. 429–437.

Fershtater, G.B., *Petrologiya glavnykh intruzivnykh assotsiatsii* (Petrology of the Main Intrusive Associations), Moscow: Nauka, 1987 [in Russian].

Fershtater, G.B., *Paleozoiskii intruzivnyi magmatizm Srednego i Yuzhnogo Urala* (Paleozoic Intrusive Magmatism of the Middle and Southern Urals), Ekaterinburg: RIO Ural. Otd. Ross. Akad. Nauk, 2013 [in Russian].

Fishman, M.V. and Goldin, B.A., *Granitoidy tsentral'noi chasti Pripolyarnogo Urala* (Granitoids of the Central Part of the Subpolar Urals), Moscow–Leningrad: Izd. Akad. Nauk SSSR, 1963 [in Russian].

Fu, B., Mernagh, T.P., Kita, N.T., Kemp, A.I.S., and Valley, J.W., Distinguishing magmatic zircon from hydrothermal zircon: a case study from the Gidginbung high-sulphidation Au–Ag–(Cu) deposit, SE Australia, *Chem. Geol.*, 2009, vol. 259, pp. 131–142.

Gerdes, A. and Zeh, A., Zircon formation versus zircon alteration – new insights from combined U–Pb and Lu–Hf in-situ LA-ICP-MS analyses, and consequences for the interpretation of Archean zircon from the Central Zone of the Limpopo Belt, *Chem. Geol.*, 2009, vol. 261, pp. 230–243.

Grimes, C.B., Joh, B.E., Kelemen, P.B., Mazdab, F.K., Wooden, J.L., Cheadle, M.J., Hanghoj, K., and Schwartz, J.J., Trace element chemistry of zircons from oceanic crust: a method for distinguishing detrital zircon provenance, *Geology*, 2007, vol. 35, pp. 643–646.

Hanchar, J.M. and Watson, E.B., Zircon saturation thermometry, *Rev. Mineral. Geochem.*, 2003, vol. 53, no. 1, pp. 89–112.

Harrison, T.M. and Schmitt, A.K., High sensitivity mapping of Ti distributions in Hadean zircons, *Earth Planet. Sci. Lett.*, 2007, vol. 261, pp. 9–19.

Hoskin, P.W.O., Trace-element composition of hydrothermal zircon and the alteration of Hadean zircon from the Jack Hills, Australia, *Geochim. Cosmochim. Acta*, 2005, vol. 69, no. 3, pp. 637–648.

Hoskin P.W.O. Trace-element composition of hydrothermal zircon and the alteration of Hadean zircon from the Jack Hills, Australia, *Geochim. Cosmochim. Acta*, 2005, vol. 69, no. 3, pp. 637–648.

Hoskin, P.W.O. and Schaltegger, U., The composition of zircon and igneous and metamorphic petrogenesis, in *Zircon*, Hanchar, J.M., and Hoskin, P.W.O., Eds., *Rev. Mineral. Geochem.*, 2003, vol. 53, pp. 7–62.

Il'yasova, G.A., Ostanin, S.Yu., Mikhaleva, E.N., et al., *Gosudarstvennaya geologicheskaya karta Rossiiskoi Federatsii. Masshtab 1 : 200000. Izd. vtoroe. Seriya Severo-Ural'skaya. List R-40-XVIII (Lopsiya). Ob"yasnitel'naya zapiska* (The 1 : 200000 State Geological Map of the Russian Federaton, 2nd ed., Ser. Northern Urals, Sheet R-40-XVIII (Lopsiya). Explanatory Note), Moscow: Mosk. Fil. Vseross. Nauchno-Issled. Geol. Inst., 2017 [in Russian].

Ivanov, V.N., Zharkova, T.B., Kurzanov, I.Yu., et al., *Gosudarstvennaya geologicheskaya karta Rossiiskoi Federatsii. Masshtab 1 : 200000. Seriya Severo-Ural'skaya. List Q-40-XXX (Manaraga). Ob"yasnitel'naya zapiska* (The 1 : 200000 State Geological Map of the Russian Federation. Ser. North Urals. Sheet Q-40-XXX (Manaraga). Explanatory Note), Moscow: Mosk. Fil. Vseross. Nauchno-Issled. Geol. Inst., 2013a [in Russian].

Ivanov, V.N., Zharkova, T.B., Kurzanov, I.Yu., et al., *Gosudarstvennaya geologicheskaya karta Rossiiskoi Federatsii. Masshtab 1 : 200000. Seriya Severo-Ural'skaya. List Q-41-XXV. (Narodnaya). Ob"yasnitel'naya zapiska* (The 1 : 200000 State Geological Map of the Russian Federation. Ser. North Urals. Sheet Q-42-XXV (Narodnaya). Explanatory Note), Moscow: Mosk. Fil. Vseross. Nauchno-Issled. Geol. Inst., 2013b [in Russian].

Kepezhinskas, P., McDermott, F., Defant, M.J., Hawkesworth, C.J., Hochstaedter, A., Drummond, M.S., Koloskov, A., Maury, R.C., and Bellon, H., Trace element and Sr–Nd–Pb isotopic constraints on a three-component model of Kamchatka Arc petrogenesis, *Geochim. Cosmochim. Acta*, 1997, vol. 61, pp. 577–600.

Kholodnov, V.V., Shardakova, G.Yu., Puchkov, V.N., Petrov, G.A., Shagalov, E.S., Salikhov, D.N., Korovko, A.V., Pribavkin, S.V., Rakhimov, I.R., and Borodina, N.S., Paleozoic granitoid magmatism of the Urals: the reflection of the stages of geodynamic and geochemical evolution of a collisional orogen, *Geodynam. Tectonophys.*, 2021, vol. 12, no. 2, pp. 225–245.

Kholodnov, V.V., Shardakova, G.Yu., Dushin, V.A., Korovko, A.V., and Shagalov, E.S., Riphean–Vendian–Cambrian magmatism of the Mankhambo Block (Subpolar Urals): Geochemical typification, correction of geodynamic concepts, and the role of plume–lithosphere interaction, *Petrology*, 2022, vol. 30, no. 4, pp. 392–417.

Kostitsyn, Y.A., Belousova, EA., Silant'ev, S.A., Bortnikov, N.S., and Anosova, M.O., Modern problems of geochemical and U–Pb geochronological studies of zircon in oceanic rocks, *Geochem. Int.*, 2015, vol. 53, no. 9, pp. 759–785.

Krasotkina, A.O., Skublov, S.G., Kuznetsov, A.B., Makeev, A.B., Astaf'ev, B.Yu., and Voinova, O.A., The first data on the age (U–Pb, SHRIMP-II) and composition of zircon from the unique Yarega oil–titanium deposit, South Timan, *Dokl. Earth Sci.*, 2020, vol. 495, no. 2, pp. 872–879.

Kuznetsov, N.B., Cambrian Baltica–-Arctida collision is the earliest stage of "assembling" the northern part of the Late Paleozoic–Early Mesozoic Pangea supercontinent, *Byull. Mosk. O–va Ispyt. Prir., Otd. Geol.*, 2009, vol. 84, no. 1, pp. 18–38.

Kuznetsov, N.B. and Udoratina, O.V., Age and geodynamic environments of the formation of the Late Precambrian granitoids of the Vangyr massif, Subpolar Urals, *Byull. Mosk. O–va Ispyt. Prir., Otd. Geol.*, 2007, vol. 82, no. 2, pp. 3–12.

Kuznetsov, N.B., Soboleva, A.A., Udoratina O.V., Gertseva, M.V., Andreichev, V.L., and Dorokhov, N.S., Pre-Uralian tectonic evolution of the north-east and east frame of the East European Craton. Part 2. Neoproterozoic—Cambrian Baltica–Arctida collision, *Litosfera*, 2007, no. 1, pp. 32–45.

Kuznetsov, N.B., Natapov, L.M., Belousova, E.A., O'Reilly, S.Y., and Griffin, W.L., Geochronological, geochemical and isotopic study of detrital zircon suites from late Neoproterozoic clastic strata along the NE margin of the East European Craton: Implications for plate tectonic models, *Gondwana Res.*, 2010, vol. 17, nos. 2/3, pp. 583–601.

Lokhov, K.I., Kapitonov, I.N., Prasolov, E.M., and Sergeev, S.A., Extremely radiogenic hafnium in the zircons from Precambrian calciphyres, *Dokl. Earth Sci.*, 2009, vol. 425, no. 5, pp. 463–466.

Loucks, R.R., Fiorentini, M.L., and Rohrlach, B.D., Divergent Ti–HO_2 paths during crystallisation of H_2O-rich and H_2O-poor magmas as recorded by Ce and U in zircon, with implications for TitaniQ and TitaniZ geothermometry, *Contrib. Mineral. Petrol.*, 2018, vol. 173, no. 12, pp. 1–21.

Makhlaev, L.V., *Granitoidy severa Tsentral'no-Ural'skogo podnyatiya: Polyarnyi i Pripolyarnyi Ural* (Granitoids of Northern Central Ural Uplift: Polar and Subpolar Urals), Ekaterinburg: Ural. Otd. Ross. Akad. Nauk, 1996.

Martin, H., The mechanisms of petrogenesis of the Archaean continental crust—Comparison with modern processes, *Lithos*, 1993, vol. 30, nos. 3–4, pp. 373–388.

Martynov, Yu.A., *Osnovy magmaticheskoi geokhimii* (Foundations of Magmatic Geochemistry), Vladivostok: Dal'nauka, 2010 [in Russian].

McDonough, W.F. and Sun, S., The composition of the Earth, *Chem. Geol.*, 1995, vol. 120, pp. 223–253.

Pearce, J.A., Harris, N.B., and Tindle, A.G., Trace element discrimination diagrams for the tectonic interpretation of granitic rocks, *J. Petrol.*, 1984, vol. 25, no. 4, pp. 956–983.

Pelleter, E., Cheilletz, A., Gasquet, D., Mouttaqi, A., Annich, M., Hakour, A.E., Deloule, E., and Feraud, G., Hydrothermal zircons: a tool for ion microprobe U–Pb dating of gold mineralization (Tamlalt-Menhouhou gold deposit—Morocco), *Chem. Geol.*, 2007, vol. 245, pp. 135–161.

Petrov, G.A., Kholodnov, V.V., Ostanin, S.Yu., Shagalov, E.S., and Konovalova, E.V., Fluid regime of formation and metallogenic features of granitoids of the Yuzhno-Pomursky Massif (Northern Urals), *Litosfera*, 2017, vol. 17, no. 5, pp. 103–112.

Puchkov, V.N., *Paleogeodinamika Yuzhnogo i Srednego Urala* (Paleogeodynamics of the Southern and Middle Urals), Ufa: GILEM, 2000 [in Russian].

Puchkov, V.N., The plume-dependent granite-rhyolite magmatism, *Litosfera*, 2018, no. 5, pp. 692–705.

Pystin, A.I. and Pystina, Yu.I., Metamorphism and granite formation in the Proterozoic–Early Paleozoic history of the formation of the Subpolar Ural segment of the Earth's crust, *Litosfera*, 2008, no. 6, pp. 25–38.

Pystin, A.I. and Pystina, Yu.I., New data on the age of granitoids of the Subpolar Urals in connection with the problem of distinguishing of the Middle Riphean Kozhim granite-rhyolite formation, *Izv. Komi NTs UrO RAN*, 2011, vol. 4 (8), pp. 73–78.

Pystina, Yu.I. and Pystin, A.I., Typomorphic characteristics of zircon as a criterion for subdivision and correlation of granitoids (on an example of the northern part of the Subpolar Urals), *Vestn. IG Komi NTs UrO RAN*, 2017, no. 12, pp. 3–15.

Rubatto, D., Zircon trace element geochemistry: partitioning with garnet and the link between U–Pb ages and metamorphism, *Chem. Geol.*, 2002, vol. 184, nos. 1–2, pp. 123–138.

Rudich, K.N., *Magma maloglubinnykh kamer* (Shallow Magma Chambers), Moscow: Nauka, 1967 [in Russian].

Rudnik, R.L. and Gao, S., Composition of the continental crust, *Treatise of Geochemistry*, 2003, vol. 3, pp. 1–64.

Semikhatov, M.A., Kuznetsov, A.B., and Chumakov, N.M., Isotope age of boundaries between the general stratigraphic subdivisions of the Upper Proterozoic (Riphean and Vendian) in Russia: The evolution of opinions and the current estimate, *Stratigr. Geol. Correl.*, 2015, vol. 23, no. 6, pp. 568–579.

Shardakova, G.Yu., Geochemistry and isotopic ages of granitoids of the Bashkirian Mega-Anticlinorium: Evidence for several pulses of tectono–magmatic activity at the junction zone between the Uralian orogen and East European Platform, *Geochem. Int.*, 2016, vol. 54, no. 7, pp. 594–608.

Sharpenok, L.V., Kostin, A.E., and Kukharenko, E.A., The alkali sum-silica diagram (TAS) for chemical classification and diagnostics of plutonic rocks, *Regional. Geol. Metallogen.*, 2013, no.56, pp. 40–50.

Soboleva, A.A., The problem of heterogeneity of the Sal'ner–Man'khambo granitoid complex, in *Geologiya i poleznye iskopaemye Zapadnogo Urala. Mater. Regional. nauchno-prakt. konf.* (Proc. Regional Sci.-Pract. Conf. "Geology and Mineral Resources of the Western Urals"), Perm: Perm. GOs. Univ., 2001, pp. 34–37.

Soboleva, A.A., *Vulkanity i assotsiiruyushchie s nimi granitoidy Pripolyarnogo Urala* (Volcanics and Related Granitoids of the Subpolar Urals), Ekaterinburg: Ural. Otd. Ross. Akad. Nauk, 2004 [in Russian].

Sun, S.-S. and McDonough, W.F., Chemical and isotopic systematics of oceanic basalts: implications for mantle composition and processes, *Spec. Publ.—Geol. Soc. London*, 1989, vol. 42, no. 1, pp. 313–345.

Sylvester, P.J., Post-collisional strongly peraluminous granites, *Lithos*, 1998, vol. 45, pp. 29–31.

Trail, D., Watson, E.B., and Tailby, N.D., Ce- and Eu-anomalies in zircon as proxies for the oxidation state of magmas, *Geochim. Cosmochim. Acta*, 2012, vol. 97, no. 1, pp. 70–87.

Udoratina, O.V., Soboleva, A.A., Kuzenkov, N.A., Rodionov, N.V., and Presnyakov, S.L., Age of granitoids in the Man'khambo and Il'yaiz massifs, the Northern Urals, *Dokl. Earth Sci.*, 2006, vol. 407, no. 2, pp. 284–289.

Udoratina, O.V., Shuiskii, A.S., and Kapitanova, V.A., Granitoids of the Kozhim massif (Subpolar Urals): U–P and Lu–Hf data, *Izv. Komi NTs UrO RAN*, 2020, no. 1(41), pp. 96–105.

Udoratina, O.V., Kulikova, K.V., and Shuyskiy, A.S., Soboleva, A.A., Andreichev, V.L., Golubeva, I.I., and Kapitanova, V.A., Granitoid magmatism in the north of the Urals: U–Pb age, evolution, sources, *Geodynam. Tectonophys.*, 2021, vol. 12, no. 2, pp. 287–309.

Volchek, E.N., *Geodinamicheskie obstanovki kislogo vulkanizma zapadnogo sektora severa Urala* (Geodynamic Conditions of Felsic Volcanism in the Western Sector of the North of the Urals), Ekaterinburg: Izd. Ural. Otd. Ross. Akad. Nauk, 2004 [in Russian].

Wang, F.Y., Liu, S.A., Li, S.G., and Yongsheng, H., Contrasting zircon Hf–O isotopes and trace elements between ore-bearing and ore-barren adakitic rocks in Central-Eastern China: Implications for genetic relation to Cu–Au mineralization, *Lithos*, 2013, vol. 156–159, pp. 97–111.

Whalen, J.B., Currle, K.L., and Chappell, B.W., A-type granites: Geochemical characteristics, discrimination and petrogenesis, *Geol. Soc. Am. Abstr. Progr.*, 1979.

Yan, Q., Zhang, P., Metcalfe, I., Liu, Y., Wu, Sh., and Shi, X., Geochemistry of axial lavas from the mid- and southern Mariana Trough, and implications for back-arc magmatic processes, *Mineral. Petrol.*, 2019, vol. 113, pp. 803–820.

Zaitceva, M.V., Pupyshev, A.A., Shchapova, Yu.V., and Votyakov, S.L., The U-Pb dating of zircons using NexION 300S quadrupole mass spectrometer with inductively coupled plasma and NWR 213 attachment for laser ablation, *Analitika Kontrol'*, 2016, vol. 20, no. 4, pp. 294–306.

Zhong, S., Feng, C., Seltmann, R., Li, D., and Qu, H., Can magmatic zircon be distinguished from hydrothermal zircon by trace element composition? The effect of mineral inclusions on zircon trace element composition, *Lithos*, 2018, vol. 314–315, pp. 646–657.

Translated by I. Melekestseva